On Heat Loading, Novel Divertors, and Fusion Reactors

M. Kotschenreuther,* P. M. Valanju, and S. M. Mahajan

Institute for Fusion Studies, The University of Texas at Austin

(Dated: March 22, 2006)

Abstract

It is shown that the limited thermal power handling capacity of the standard divertors (used in current as well as projected tokamaks) forces extremely high ($\sim 95\%$) radiation fractions f_{Rad} in tokamak fusion reactors [1–3] with heating powers considerably larger than ITER-FEAT [4]. Independent of how the radiation may be apportioned between the scrape off layer (SOL) and the core, these enormous values of f_{Rad} have profound and deleterious consequences on the core confinement and stability to the extent that a high power hypothetical fusion reactor operating with the standard divertor (SD) is not likely to meet the daunting confinement requirements. Even operation in modes that have an internal transport barriers (ITBs) [5, 6] is not expected to lead to a dependable fusion power reactor with acceptable economics.

The core confinement and stability problems caused by high f_{Rad} are shown to be adequately addressed by X-Divertors (XD) which, through a flaring of the field lines near the divertor plates, considerably enhance the divertor thermal capacity. The use of this new class of divertors will lower the bar on confinement sufficiently that confinement at the level of the routinely found H-mode [7] could be enough for a fusion reactor. A possible class of experiments that could lay the foundation for an efficient and attractive path to practical fusion power is suggested.

PACS numbers:

I. INTRODUCTION

Although the heat loading issues pertinent to an economical tokamak Deuterium-Tritium (DT) fusion power reactor have occupied some space in the magnetic fusion discourse [1–3, 8], their seriousness and possible severity has not been critically examined. For the current large-scale experiments (ASDEX [9], DIII-D [10], JET [11], JT60-U [12], etc), heat loading puts no severe constraints on the machine operation. In the much bigger planned burning plasma experiment (ITER-FEAT, fusion power $P_F = 400$MW) [4, 13, 14], the heating power (P_{Th} ∼120 MW) reaches high enough levels that its appropriate handling can, no longer, be ignored (a well-recognized fact taken into consideration by the designers of ITER [15]). For any economically power producing magnetic fusion reactor, however, the heating powers are *significantly* larger. The heating power P_{Th} in the conservative European Union fusion reactor EU-B ($P_F = 3600$MW) [1, 16], for example, is ∼ 990MW which is about 8 times larger than ITER-FEAT. The problems associated with handling such prodigious amounts of heat without destroying its components force a fusion reactor into a physical regime (characterized by high radiation requirements primarily in the core) very different from the one pertinent either to the current machines or to ITER. Novel solutions will have to be invented in order to bring the radiation fraction to a manageable level so that the high core plasma performance required for sustained fusion can be achieved and maintained.

A straightforward assessment (carried out in Sec.II) of the heat handling capacity of the standard divertor (SD), the divertor configuration used in present tokamaks and the proposed ITER-FEAT [17], reveals that the thermal power loads relevant to a fusion reactor are about an order of magnitude more than the rather limited capabilities of the SD. The key measure of the divertor heat rating is P_{plate}, the maximum thermal power that the divertor plate can handle. It is limited by stringent material and engineering constraints (∼10 MW/m^2) and the geometry of the standard divertor (SD), which concentrates the exhausted power onto the divertor plate. The tendency for the heat flux to become concetrated on the divertor plate is a fundamental consequence of the transition from closed field lines to open field lines, together with the very rapid parallel transport in hot plasmas. The concept of a "magnetic bottle" is to maintain a hot thermonuclear plasma while the material container of the plasma stays under acceptable conditions. One message of this paper is that these necessary conditions for a viable magnetic bottle are violated for reactor power levels with

the standard divertor (SD) configuration. For the standard divertor, the only way to maintain an acceptable condition for the wall is to radiate a huge fraction of the heating power. We will show that the fraction of the heating power which is radiated f_{Rad} must be of order $\sim 95\%$ for a fusion reactor with a standard divertor (SD).

Independent of how the necessary radiation is apportioned between the divertor/scrape off layer (SOL) and the core plasma, such a high f_{Rad} has profound damaging effects on the core energy confinement and stability of a burning plasma. Working out consequences of high f_{Rad} forms the bulk of the argument in Sec.III against the suitability of the SD for a fusion reactor, and allows an assessment of what f_{Rad} may be tolerable. The analysis in this paper is based primarily on the existing experimental and modeling results.

The general analysis yields an important positive result (delete:of fundamental importance): the core plasma confinement and stability will remain "healthy" if the radiation fraction f_{Rad} falls to $\sim 75\%$ or below, and furthermore, the divertor magnetic geometry can be improved to reduce f_{Rad} to the desired range. The substantial changes in the magnetic geometry of the divertor which are examined here have not been considered possible or necessary before. The new divertor geometry (which we shall call X-Divertor, or XD, to distinguish it from the standard divertor, or SD) will, therefore, lead to the substantial, and probably crucial, improvements in the overall feasibility of fusion reactor.

One major ingredients of our analysis is the demonstration that the main strategy currently envisaged for handling high power levels, that is, increasing the radiative ability of the SOL (we include the divertor region in SOL) by seeding it with low Z impurities [17] probably won't succeed for a reactor. It will be demonstrated that, when impurity levels are increased to radiate large reactor-relevant powers in the SOL, one ends up radiating most of the power from the core. Relative to the total radiation demands in a reactor with SD, the reactor SOL has a limited radiative capacity (via impurities).

The most spectacular but negative consequence of the limited heat handling capability of the SD (forcing high f_{Rad}) is the termination of the experimentally demonstrated robust and consistent favorable scaling (towards self-sustained thermonuclear reactions) with size, magnetic field and power level. It is this empirical trend that has propelled fusion advancement from the first tokamak to JET, JT60, and TFTR. When appropriately quantified and scaled, this trend predicts that ITER-FEAT will achieve high energy gain [4, 14]. We show in Sec.III that this trend reverses if one persists with the standard divertor (SD) - an

unfavorable trend in confinement begins for power levels higher than ITER-FEAT.

The damaging effect of the required high radiation on the overall energy confinement is small and acceptable for ITER-FEAT. Empirical, gyro-Bohm scaling of H-mode plasma transport from present tokamaks suffices to achieve high fusion gain at ITER-FEAT power levels [7] (gyro-Bohm scaling refers to the scaling of plasma transport with ρ^* = the ion gyroradius divided by the system size, and ρ^* is the primary dimensionless physics parameter that distinguishes ITER from present experiments). For reactors characterized with much higher thermal power than ITER-FEAT, on the other hand, the radiation requirements become so high that the core confinement is seriously degraded.

Could operation with internal transport barriers (ITBs) [5, 6] attain the high confinement required for reactors with the standard divertor (SD) and the accompanying high f_{Rad}? Based on available experimental results and theoretical calculations, we show in Sec.IV A that even ITBs are not likely to rescue the SD reactor; the confinement needs for a reactor relevant plasma, when compared to what is achieved in present experiments, are rather severe. In Sec.IV B, we further show that even if it were somehow possible to obtain ITBs with high enough confinement, the plasma transport will most likely be too low for adequate helium exhaust - the result will be a radiation collapse of the core inside the ITB.

In Sec.V, we show that a self-heated fusion plasma is thermally unstable in the presence of a high core radiation fraction $f_{Rad,Core}$. The results are rather sobering; at the high $f_{Rad,Core}$ forced by a standard divertor (SD), the thermal instability is sufficiently virulent that feedback methods appear unworkable. The instability is even stronger for ITB plasmas. One expects that a virulent thermal instability is to be avoided for a power reactor.

The challenge, therefore, is to find ways to bring f_{Rad} down to a manageable level. The solution has to be found in the divertor geometry since there is not much play in other plasma variables. (Note that liquid metal divertors [18–20] with a higher heat flux capacity may also be used; the liquid metal divertors are compatible with the new geometries discussed. In fact, the new X-divertor (XD) geometries may make them easier.) From a variety of possible magnetic geometries recently investigated [21–23], we present in this paper (Sec.VI) a class of new divertors (which we call X-divertors, or XD) whose power rating is considerably increased by creating additional X-points to flare the field lines just before they strike the divertor plates (see Figs.11-12). These new X-divertors lower the bar for core confinement to an extent that scaling poorer than gyro-Bohm will turn out to be sufficient for a fusion

reactor. With radiation fraction down to a manageable level, the robust favorable scaling with machine size and power level becomes available once again even for machines with power levels much beyond ITER-FEAT.

Clearly, the new X-divertor (XD) needs to be subjected to rigorous experimental tests before implementation in a reactor. In fact, there is a fortunate symbiosis between the proposed X-divertor (XD) concept and a Component Test Facility (CTF) [24] (discussed in some detail in Appendix G). A CTF is recognized as a critical step for developing the fusion technology necessary for a reactor. It is shown in Appendix G that a CTF is not possible with a standard divertor (SD), but will become possible with the new X-divertor (XD). A CTF-XD can also play a critical role in the physics development of fusion, by demonstrating the workability of new X-divertor under reactor-like conditions. If the new X-divertor does what it is expected to, it will be relatively straightforward to scale CTF-XD to a reactor - make it larger, and rely on the favorable scaling with size, field and power.

In Sec.VII, we sum up our findings including our suggestions for future experiments.

II. REACTOR POWER HANDLING LIMITS - HIGH RADIATION FRACTION

The total thermal power capacity, P_{plate}, of the divertor plate of a reactor is proportional to the maximum MW/m^2 (q_{max}) that its design can withstand, and the plasma-wetted area A_w which increases with the major radius R. Out of these controlling factors, the size R is strongly limited by economics, or equivalently, by the need for adequate wall loading. The material and engineering constraints (under reactor conditions) set a stringent and inviolate upper bound on the steady state q_{max} which must remain below 10-15 MW/m^2 [1, 25, 26]. It is considered highly unlikely that this limit will significantly increase in future - even 10MW/m^2 is regarded as optimistic, perhaps speculative in the high neutron fluence of a power reactor [1, 25, 26].

The plasma-wetted surface area A_w at the divertor plate equals [27]

$$A_w = \frac{4\pi R}{\sin(\theta_t)} W_{SOL} F_{exp} \tag{1}$$

where W_{SOL} is the width of the scrape off a layer at the mid plane, F_{exp} is the flux expansion at the divertor plate, and θ_t is the angle of incidence of the poloidal field with the divertor plate. For this calculation, $\theta_t = 25$ degrees (the value used in ITER) will be assumed.

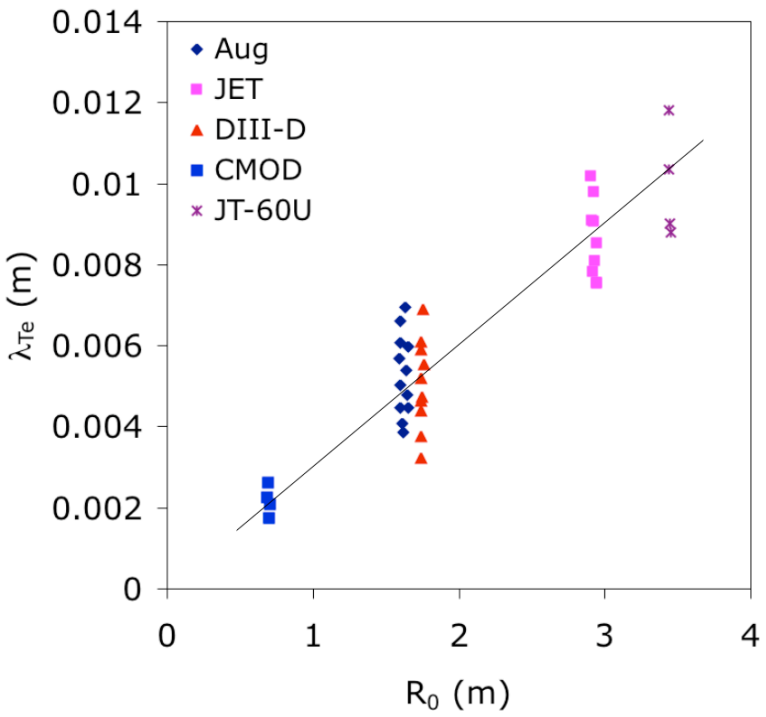

FIG. 1: SOL width λ_{Te} verses major radius $R0$. Data from Kallenbach, et.al. [31]

Equation 1 optimistically assumes that the heat is distributed evenly between the inner and outer divertor, though JET experiments show that the power to the inner divertor is much less than the outer divertor [28]. It should be noted that simulations of partially detached regimes for ITER scenarios find that a smaller θ_t gives only small improvements [29] or no improvement [30] in the heat flux to the plate; Eq.1 is no longer valid for low enough θ_t.

For W_{SOL}, we use data drawn from [31] and displayed in Fig.1, where the thermal width λ_{Te} of the SOL is plotted against the major radius. This shows $\lambda_{Te} \sim R$; its dependence on other parameters is statistically insignificant in this data set. The width over which the power flows out (the quantity of direct relevance here) is 2/7 of the SOL temperature width λ_{Te} [27, 31]. Thus the power width at the outboard mid plane of the SOL is $\sim 8 \times 10^{-4} R$. This can be reasonably extrapolated to reactors with R=5.4-8.6 m. For ITER-FEAT (with P=400 MW, and total thermal power, P_{th}=120MW), we find W_{SOL}=0.005 m. The formula used here yields results that agree with other methods used to project W_{SOL} for ITER. Comprehensive 2D divertor simulations of the ITER divertor [13] also give a W_{SOL} of roughly 0.005 m. The power width was investigated on JET [28], and the best fit of the experimental data led to an expected W_{SOL} of 0.0037 m for ITER - fairly similar to 0.005 m.

Free boundary MHD equilibria using the code FBEQ [32] with the ITER coil set obtain a flux expansion of 4.3 (which is also typical of equilibrium reconstructions on JET [28]). Equation 1 then gives A_w=4 m^2. For a maximum heat flux of 10 MW/m^2, this divertor plate has a maximum P_{plate} rating of 40 MW (similar to the ITER-FEAT design based on older data [33]). Naturally the remaining 80MW (=120-40) MW, constituting $\sim 67\%$ of the thermal power, must be radiated away before arriving at the divertor plate.

Moving on to reactors, we first consider the European Union design EU-B [1, 16], based on an avowedly conservative extrapolation of ITER-FEAT H-mode operation. The EU-B has P=3600MW, R=8.6m, and P_{Th}=990MW, and an estimated cost of electricity $\sim 20-30\%$ higher than reactor designs based on Advanced Tokamak (AT) operation studies for ARIES-RS, EU-C, and CREST [1–3]. Using Eq.1 and Fig.1, A_w=7.7 m^2, and P_{max}(EU-B)=77 MW. Notice that the maximum tolerable divertor power, P_{max}, has increased only modestly in going from ITER to EU-B (since the major radius is only $\sim 40\%$ larger) while the thermal power to be handled has gone from 120MW to a stupendous 990MW. In order to avoid destroying the divertor, therefore, the EU-B will have to operate at a radiation fraction of $\sim 92\%$. For other reactor designs, including ARIES RS [2] and CREST [3], the fractions range from $\sim 92\%$ to 96%, as shown in Table I. The average radiation fraction for these four studies is $\sim 94\%$. If most of the power were to go to the outer divertor (consistent with experimental results on JET [28]), the required radiation fractions would lie in the range $94\%-98\%$. What happens to a reactor when $\sim 95\%$ of its heating power has to be radiated away is the question that we attempt to answer in the next section.

III. HIGH RADIATION FRACTION - DEGRADATION OF PLASMA PHYSICS

Radiation of excess thermal power ($\sim 95\%$ of the total) is essential for avoiding divertor destruction in reactors. In principle, one could attempt to operate the discharge either by radiating mostly in the divertor/SOL region, or by radiating in the core. Unfortunately, the physics of the discharge is very adversely affected no matter which option (or combination of options) is tried. The deleterious effects of a high radiation fraction are numerous and can cause damage (loss of confinement, disruptions, core thermal instability, loss of staying in H mode, pressure profiles with low beta limits, etc.) through many channels. Any one of these channels could destroy the reactor workability. This section, therefore, has many

sub-sections in which each of these channels is explored in some detail.

If most of the power could be radiated in the SOL, then one may expect that core confinement would not be seriously affected and one could extrapolate the core physics from present experiments and ITER to a reactor. It makes sense, then, to examine if the SOL can pick up the lion's share of radiation. In the following three sections, a detailed case is made for the near impossibility of radiating large fractions of power in the SOL. In Sec.III A, we show that the current paradigm for creating high radiation fraction in SOL, through a seeding of the discharge with low Z impurities, is not likely to scale to reactor needs, even though this approach seems to work for the present machines. Numerous and disabling problems with the remaining option for radiating a large fraction of the power in SOL (to have a high SOL neutral density with full divertor detachment) are discussed in Sec.III B.

A. Impurity driven SOL radiation - unfavorable scaling to a reactor

The strategy of preferentially enhancing divertor radiation (without affecting the core) with impurities has been used with some success in present experiments [34, 35]. The nature of the underlying physical processes, however, does not allow the impurity driven radiation to be localized in SOL for devices with larger size, higher temperatures and higher power levels. For reactors, adding low Z impurities to enhance divertor radiation ends up with putting much higher amount of radiation in the core plasma than in the divertor. This claim will be supported by two lines of arguments - from the scaling of the underlying physics, and from empirical scaling results.

Although the SOL radiation occurs near an optimal temperature (< 30eV) determined by atomic physics, the radiating efficacy of the SOL in a reactor will be quite different form present experiments. This happens because a much lower fraction of the divertor volume is at the optimal radiating temperature in a reactor. The SOL temperature in contact with the main plasma is too high for optimal radiation (T $\sim$ 80eV in JET and $>$ 200eV in a reactor). The fraction of the SOL at temperatures $<$ 30eV is much smaller in a reactor, hence the useful radiating volume is much less. Using the two-point model [27], the radiating efficacy of the SOL scales roughly as $T^{-3/2}$ [Appendix A]. However, the two-point model ignores convection, and experimentally, convection has been found to be important for highly radiating divertors [36]. Nonetheless one can derive a scaling procedure

from current experiments to reactors as follows. By including convection in the two-point model, the equation for the temperature along a field line can be derived. The structure of the resulting solution allows (for the same impurity level) the scaling of the impurity SOL radiation from current experiments to a reactor (See Appendix A). For a given impurity level, the SOL radiation should scale as

$$P_{Rad} \sim R W_{SOL} n_{SOL}^2 \tag{2}$$

This yields the ratio of the core radiation from Bremsstrahlung to the SOL radiation

$$\frac{P_{core}}{P_{SOL}} \sim \frac{a^2 n_{core}^2 \sqrt{T}}{W_{SOL} n_{SOL}^2} \tag{3}$$

where a is the minor radius, T the core temperature, and n_{core} and n_{SOL} are the core and SOL densities, respectively. This ratio increases with machine size and core temperature. Both of these are larger on a reactor. Recent results indicate that core density peaking is also expected to be much larger for reactors operating near the Greenwald limit [37–39] as compared to present experiments near that limit (reactors will have much lower collisionality). All these factors conspire to make the ratio of the core to SOL impurity radiation to be over an order of magnitude larger on a reactor as compared to present experiments (see Appendix A for more detailed comparisons).

In experiments with low Z seeding on JET for ITER-relevant discharges with a total radiation fraction of $\sim 70\%$, the ratio of core to SOL radiation can be as low as ~ 0.4 [34]. For the smaller and cooler DIII-D, Eq.3 predicts the core to SOL ratio to go down by a factor of about 2. Experiments with a total radiation fraction of $\sim 70\%$ have, indeed, attained a ratio ~ 0.25 [35]. The same scaling predicts that for a reactor the core radiation will be several times the SOL radiation.

The experiments we have discussed so far are not in the $f_{Rad} \sim 95\%$ range. One could, perhaps, expect reaching higher levels of SOL radiation by increasing the impurity fraction. Experiments on DIII-D (Fig.2), however, show that beyond some level, the SOL radiation increases much more slowly with increasing impurities than does the core radiation; the increased radiation shifts to the core at high impurity levels. As indicated in Appendix A, this is consistent with the two-point model with convection - the SOL impurity radiation should saturate with increased impurity concentration.

Thus a reactor can be expected to have a substantially higher ratio of core to SOL

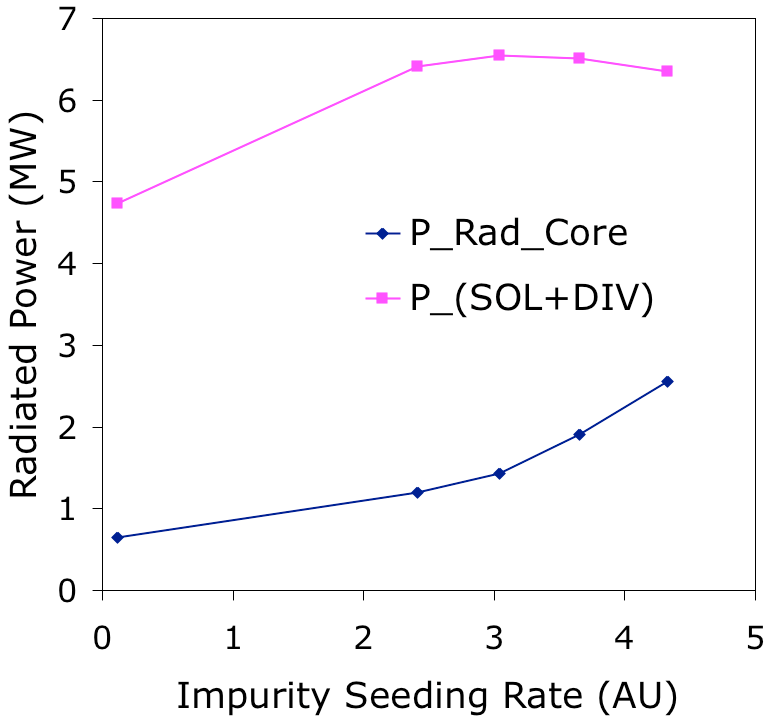

FIG. 2: SOL radiation increases much more slowly with increasing impurities than core radiation. Data from Wade, et al. [35].

radiation both because of the unfavorable scaling of SOL radiation with size and because of the very high radiation fractions needed.

Experimental results also indicate that core radiation becomes more dominant as reactor regimes are approached. As part of the experimental program leading up to ITER, Mathews [40] examined a large number of discharges with low Z impurity seeding to radiate the heating power and to reduce divertor heat loads. In most of these experiments, the radiation came primarily from the SOL, but in some cases it was mainly from the core. An empirical expression was developed to predict the core contamination for ITER from the radiated power from all sources

$$Z_{eff} = 1 + 5.6 Z^{0.19} P_{rad} / S^{1.03} n_e^{1.95} \tag{4}$$

where Z_{eff} is the core value of the effective ion charge, P_{Rad} is the radiated power in MW, S is the plasma surface area, and n_e is the average density. For many present experiments, Eq.4 is consistent with radiation predominantly from the SOL. However, when applied to EU-B with radiation equal to $\sim 93\%$ of the heating power (920MW), this formula predicts very high Z_{eff} with low Z impurities. For seeding species Ne or Ar, the Z_{eff} is 4.3 and 4.7,

respectively. Using H-mode like profile for a reactor, with the same average temperature as EU-B (see Appendix C), the core radiation power from this Z_{eff} is high ($\sim 100\%$ to $\sim 200\%$ of the heating power, depending upon the Helium fraction. Numbers in the upper range are most consistent with quoted EU-B parameters [1, 16]).

This empirical formula may be expected to have significant errors when extrapolated so far, but nonetheless it indicates that high radiation fractions for reactor parameters will arise mainly from the core. Some results from DIII-D [35] have roughly half of the $Z_{eff} - 1$ implied by Eq.4 but even this gives a high core radiation fraction, and, as indicated above, these results do not extrapolate favorably to reactors with higher radiation fraction.

It is worth noting that the ITER team does not consider cases with large fractions of low Z impurities because the resulting Z_{eff} is considered unacceptable [13]. However, a large divertor neutral pressure can cause large radiation in a fully detached plasma even for a reactor [13]. Full detachment, in which plasma is separated by a neutral gas target layer from the divertor plate, is considered in the next section.

B. Radiating in the divertor/SOL - Loss of H-mode, Disruptions

Experiments trying to maintain good H-mode confinement along with significant SOL radiation are found to lie in the partial detachment regime [41]. Although the relatively modest radiation requirements on ITER-FEAT [33] may allow it to radiate substantially in the SOL (in the partially detached H-mode phase), this choice will not be available to devices with higher power (higher radiation requirement).

When experiments proceed beyond partial plasma detachment to full detachment, divertor heat fluxes are greatly reduced and radiation levels are increased. However, the current experimental results on H-mode discharges that are fully detached are broadly and deeply discouraging. Experimental results show that full detachment leads to: 1) very poor H-mode confinement (closer to L-mode), 2) total loss of H-mode, and 3) high disruptivity. In Appendix B, we present the experimental evidence in more detail. Here, we simply note that full detachment is not regarded as a viable regime for ITER [13, 42].

We now examine quantitatively how large SOL radiation affects reactor operations. For this purpose, we will rely on the ITER divertor design team publications based on 2-D simulations by Kukushkin, et al. [13, 15, 29, 30, 43], which are by far the most extensively

developed and well-benchmarked calculations currently available for reactor-relevant burning plasmas. The simulation results clearly indicate that full divertor detachment will be necessary to maintain the peak heat flux below 10 MW/m^2 [13] if excessive power is transported into the SOL from the core. These investigators also present quantitative results in a form that is intended for extrapolation to ITER-like reactors.

Device Name, and Type: Reactor/BPX Divertor: SD/XD	**Heating Power P [MW]**	**Major Radius R [m]**	**P/R** [MW/m]	**Total** f_{Rad} (ITER-like)	**Minimum Core** f_{Rad} (Avoid detachmant)
ITER-FEAT (BPX SD)	120	6.2	19	75%	16%
ITER-EDA (BPX SD)	300	8.2	37	87%	56%
EU-B (Reac SD)	990	8.6	115	93%	86%
EU-C (Reac SD)	792	7.5	106	94%	85%
EU-D (Reac SD)	571	6.1	94	95%	83%
ARIES-RS (Reac SD)	515	5.5	94	95%	82%
CREST (Reac SD)	691	5.4	128	97%	87%
ARIES-XD (Reac XD)	515	5.5	94	$\sim$ 74%	47%
EU-B-XD (Reac XD)	990	8.6	115	$\sim$ 79%	58%
CREST (Reac XD)	691	5.4	115	$\sim$ 79%	62%

TABLE I: Necessary radiation fractions for divertor survival (assuming that a good H-mode edge is required). Only reactors with the new X-Divertor (XD) have total f_{Rad} comparable to ITER-FEAT, and manageable core radiation fractions.

Our quantitative arguments draw on the results of [13] that span a large parameter range, and have also provided the basis for the ITER divertor design. For ITER, a maximum of about 120 MW can be lost into the SOL without resorting to full detachment to prevent divertor damage. Since the major radius of reactors is only slightly different than ITER's, the maximum power for reactors is in a similar range, which is far less than the total heating power. Also, since full detachment has highly undesirable consequences, it would be desirable to operate slightly below it. Thus, we adopt 100MW as the practical maximum power which could flow into the SOL and have heat fluxes below 10 MW/m^2.

Thus, ITER-FEAT, is roughly at the limit where one can maintain good confinement

while isolating the required radiation mainly in the SOL. For a higher power device, much of the radiation burden must be shifted from the SOL to the plasma core if we want to avoid full detachment and keep a good H-mode and at the same time not subject the divertor plate to technologically unacceptable heat fluxes. Kukushkin also recommends an approximate procedure to extrapolate his results to a reactor [13], which is used here to obtain the quantitative results for various reactor designs shown in Table I.

C. Radiative capacity of SOL - Separatrix density

Since the radiative capacity of the SOL is roughly proportional to density squared, it suffers a reduction with a decrease in density. Unfortunately, at higher edge density the H mode is often lost implying an operational density limit. The density limits tends to further restrict the SOL ability to radiate.

ITER, for instance, is intended to operated with pedestal density $n_{ped} \sim 0.85 n_G$ [33], where n_G is the Greenwald density limit. However, recent experiments on JET and ASDEX show that the n_{ped} at which H-mode is lost is often much less (Fig.3). Confinement quality at the level of an H-mode is required for a fusion reactor [1–3, 8]. From the available data, Borass has arrived at a theoretically motivated scaling law for the maximum pedestal density [44]. More recent JET results have verified the parametric dependence of his empirical scaling [45], which also agrees with data for Helium discharges [46]. For ITER and the reactors, the maximum pedestal density as predicted by the scaling law turns out to be about half the Greenwald density. This would further decrease the capacity of the SOL for radiation (below the already small values in Table I) , and thereby increase the need for core radiation.

The main message of Secs.III A-III C is that the radiative capacity of a reactor SOL is severely limited, falling seriously short of the enormous radiation requirements for reactors with a standard divertor (SD). To develop an appreciation for the disparity between the large amounts of thermal power that must be radiated (P_{Rad}) and relatively modest capacity of SOL to radiate (P_{SOL}), we reproduce some numerical examples from actual reactor studies [1, 2, 16]. For the EU-B, the total plasma heating power P_{Th} is 990 MW with a P_{Rad}~920. The predicted maximum P_{SOL} for this ITER-like configuration comes out to be 139 MW. For EU-C, the EU design in the AT (ITB) mode, P_{Th} ~792 MW with P_{Rad}~744. Present experimental results show that an H-mode edge is necessary to obtain reactor relevant β_N

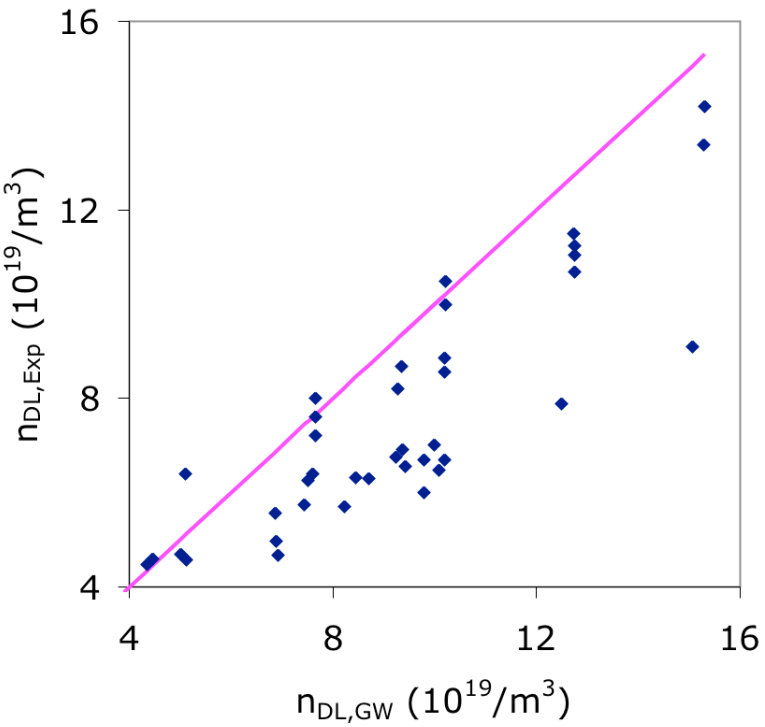

FIG. 3: Experimentally determined density limit for H to L transition verses the Greenwald density limit on ASDEX-U and JET. Note that the H-mode density limit is often considerably below the Greenwald limit (∼0.5). Data from Borass, et al. [44].

for an ITB plasma. This brings EU-C within the purview of SOL radiation limits which yield a maximum P_{SOL}∼121 MW. Similarly, we find that for ARIES-RS, the corresponding values are P_{Th} ∼515 MW, P_{Rad}∼490, and P_{SOL}∼90 MW. The (P_{Rad}, P_{SOL}) = (920,744,490) and (139,121,90) exposes a stunning disparity. In contrast, the ITER-FEAT situation is dramatically different; for this device, P_{Rad}∼85 MW is slightly smaller than the maximum P_{SOL}∼100 MW, so the SOL can radiate most of the power.

D. Radiating in the Core - Loss of Power

Since the thermal power radiated by the SOL/divertor of a reactor cannot be arbitrarily large (without causing unacceptable confinement degradation), the plasma core must pick up the slack if the reactor is to function without destroying the divertor. It is natural to expect that any radiation from the core would adversely affect core energy confinement unless somehow the energy loss via plasma transport is decreased. In spite of the widespread

belief that the core radiation reduces the energy confinement, predictive models of the effects of core radiation on confinement have not been quantitatively formulated. Based on experimental results and theoretical reasoning, such a model is formulated in Appendix C. We state the principal elements of the model and then go on to discuss its predictions.

The model is based on the following observations: 1) the core radiation clearly reduces the transport power flowing through the H-mode pedestal, 2) pedestal pressure is observed to depend on transport power in many experiments, 3) it is well accepted that the pedestal pressure strongly affects core confinement in experiments (also predicted by stiff ion temperature gradient [ITG] models of transport [47–49], and 4) thus, a reduction in pedestal pressure with reduced transport power would lead to lower stored energy. We find that the effects of core radiation can be incorporated by following the simple rule: when scaling laws are used to predict stored energy, the heating power should be taken to be the absorbed input heating power minus the core radiation power. This results in an effective reduction for stored energy by the factor $(1-f_{Rad,Core})^{0.31}$. This is entirely equivalent to adjusting the confinement enhancement factor $H_H = \tau_E/\tau_H$ downward by $(1-f_{Rad,Core})^{0.31}$. Here τ_E is the confinement time due to plasma transport (i.e., based on the heating power with radiation subtracted), and τ_H is the H-mode energy confinement time predicted by the ITER98H(y,2) gyro-Bohm scaling law [4]. Using the downward adjustment of the stored energy, quantitative prediction of the enhancement factor $H_H = \tau_E/\tau_H$ required to compensate for the loss of stored energy by radiation becomes possible. For high power machines, the calculated H_H is plotted versus the fusion power P_F in Fig.4.

The SD devices - the machines that operate with the standard divertor, are the first objects of attention. Consider a sequence of reactors with increasing major radius R (and thus fusion power P_F) but with the same dimensionless parameters as ITER (e.g. β_N, aspect ratio, safety factor q, energy multiplication Q, Impurity fraction, ratio of density to the Greenwald limit, etc.). The B field is nearly constant, but increases slightly with major radius R due to engineering considerations quantified in reactor studies (see Appendix D). We include a nominal minimum core radiation fraction of $\sim 30\%$, and when necessary, the core radiation is increased to stay below the maximum tolerable P_{SOL}. Kukushkin et al. [13] recommend scaling P_{SOL} linearly with R, which allows us to calculate P_{SOL} = (core heating power core radiation loss power), and hence the required H_H, for a given R. The blue line in Fig.4 shows the required H_H versus the total Fusion Power P_F for the sequence of SD

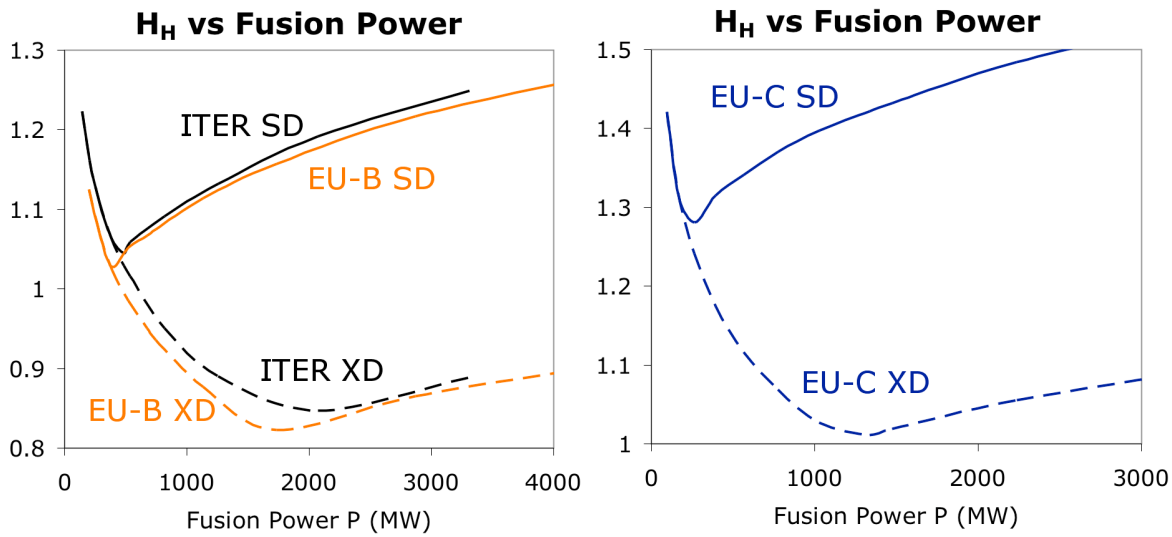

FIG. 4: Necessary confinement improvement H_H vs fusion power P. The required H_H is lower for devices with the new X-Divertor (XD) than for devices with the standard divertor (SD) for fusion power above the $\sim$ 500 MW of ITER-FEAT (see Table.1).

devices. For low powers, the required confinement is higher than H-mode, and by increasing the size and power of the device, the required confinement reaches the level of an H-mode (as predicted by the empirical scaling law). This is the robust experimental trend that "bigger size and power are better". Notice that 400 MW ITER-FEAT lies very close to the minimum of the H_H verses P_F curve, i.e, the favorable fusion scaling with power persists up to ITER-FEAT. What is even more striking is that for devices with standard divertors, the trend reverses at powers higher than ITER-FEAT; the H_H requirements become more demanding and assume very challenging values as we approach a 3000 MW fusion demonstration reactor (DEMO).

We repeat the same procedure for the corresponding devices with the new X-Divertors (XD) with considerably enhanced heat handling capability. The maximum tolerable power into the SOL is about three times higher for the new divertors, as shown in section VI.

The substantial reduction in the amount of excess power wasted via core radiation ends up reducing the required H_H for this class of machines. Consequently, the time-tested favorable scaling with power, which is denied to SD machines more powerful than ITER-FEAT, is restored for XD machines that use the new X-divertor (Fig.4).

For H-mode reactors, the XD allows operation for confinement somewhat poorer than

the nominal H-mode. With the SD, confinement would have to be substantially better than H-mode. For an AT reactor, confinement marginally better than H-mode is required, while in contrast, the SD devices have the very challenging task of making sure that their confinement is considerably better than H-mode. As we will see in section IV, it is unlikely that operation with an ITBs and a high radiation fraction is possible.

E. High Core Radiation and the L-H threshold

The high core-radiation fraction will often cause the transport power to fall perilously close to the threshold power P_{LH} necessary to maintain H-mode. In the close vicinity of P_{LH}, JET H-modes are poorly confined since Edge Localized Modes (ELMS) of type III [50] occur near threshold, and are accompanied by confinement degradation [51, 52]. Good H-mode confinement in JET (i.e. equal to the predictions of the ITER98H(y,2) scaling law [4, 14]) requires transport power $> 1.55 P_{LH}$ at high triangularity [51]. Although ITER-FEAT power is above the current empirical scaling of the P_{LH} threshold by somewhat more than a factor of 1.55, enhanced radiation fraction will make the corresponding SD reactor (H-mode EU-B, for example) fall below this requirement. On JET, the consequence of this loss is $H_H \sim 0.75$ - far below the required $H_H \sim 1.2$ needed for the EU-B reactor. It is important to also note that in a predominantly self-heated high-Q reactor, even a tiny shortfall in energy confinement (H_H) causes an unacceptably large drop in fusion power.

In contrast, all reactors with the proposed new X-Divertor (the XD branch in Fig.4) are well above 1.55 P_{LH} because they are not forced to waste power to save the divertor.

A more urgent and far-reaching consequence of the performance deterioration with a high core radiation fraction $f_{Rad,Core}$ is that the good H-mode ITER-FEAT experiments will not be able to explore the high radiation regime pertinent to a reactor ($f_{Rad,Core} \sim 85\%$). The transport power in ITER falls below 1.55 P_{LH} at a core radiation fraction $\sim 40\%$ (yielding poor H-modes), and below P_{LH} at a fraction $\sim 60\%$. In this regime, ITER is no longer a burning plasma experiment, since the confinement is not adequate to result in fusion power greater than the external heating power. Thus, one cannot expect ITER-FEAT to provide the data pertinent for a confident extrapolation to a burning plasma SD reactor with the very high core radiation fractions required to save the standard divertor.

F. Experiments at high radiation fraction

The phenomenon of confinement degradation caused by high f_{Rad} is amply supported by current experimental results. There do exist experiments in which high radiation fractions are achieved, but most such experiments do not lead to a reactor-grade plasma (not enough confinement or low β_N). A short summary of the pertinent experiments follows.

When JET plasmas radiate more than $\sim 65\%$ of the input power (total radiation in the core plus divertor), confinement drops from a good H-mode to halfway between the L and H modes ($H_H \sim 0.75$) [34]. Confinement degrades when ELMs change to type III. Ever since the ITER-EDA identified power exhaust as an issue, JET has encountered difficulty demonstrating good H-mode confinement concomitant with high radiation. This lack of success after such a great effort suggests the existence of a fundamental problem that might need a fundamentally different solution.

JT-60 has demonstrated good H-mode confinement with $\sim 80\%$ total radiation, but with $Z_{eff} \sim 4$ and thus serious plasma dilution [53]. Radiation loss fractions $\sim 95\%$, still, remain to be demonstrated on H-modes.

In the RI modes on TEXTOR, extremely high f_{Rad} ($\sim 95\%$ of the input power) have been obtained along with H-mode levels of confinement. It has not been possible, however, to reproduce their equivalent on the larger, more reactor-relevant JET. This was attributed to a lack of adequate core fueling [54], which will be even more severe in a reactor. In addition, the TEXTOR RI modes had highly peaked pressure profiles [55] implying poor ideal beta limits; the experimental achieved beta limit $\beta_N \sim 2$ [56] is much below the reactor range.

In conclusion, current experiments do not indicate a credible way of operating a reactor with a total radiation fraction $f_{Rad} \sim 95\%$ in an H-mode with good confinement ($H_H \sim 1$ or higher) and acceptable β_N.

IV. ARE REACTOR ITB'S COMPATIBLE WITH STANDARD DIVERTORS?

Having shown that the H-mode reactors are not likely to function under the severe conditions brought about by high radiation fraction $f_{Rad} \sim 0.95$ (imposed by the rather limited heat-rating of the SD), we move on to explore whether operation in an ITB mode can provide high enough confinement needed for an SD reactor which must radiate $\sim 95\%$ of its

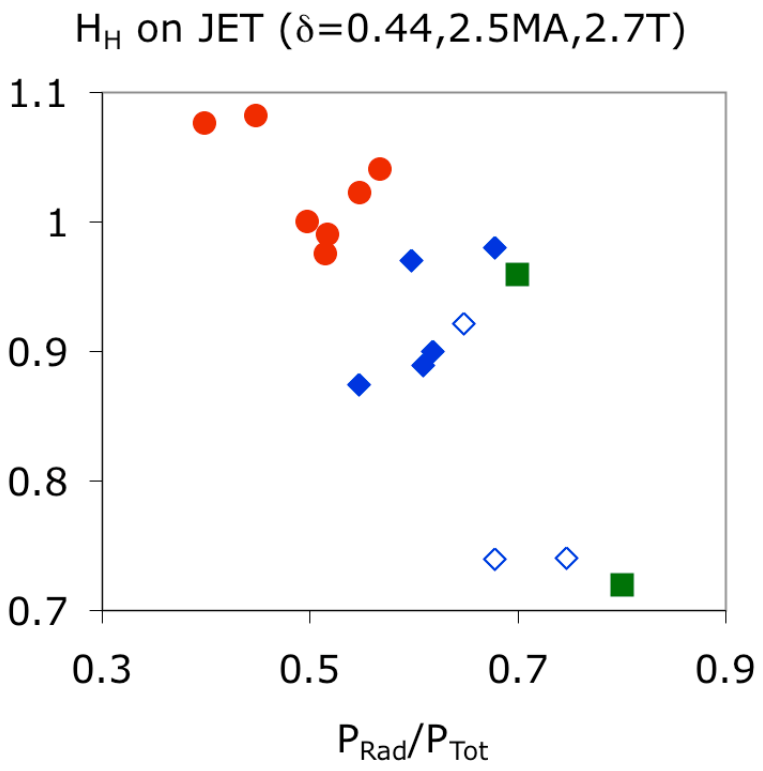

FIG. 5: Degradation of confinement with increasing radiation fraction at high density on JET. Good H-mode confinement is lost for the nominal radiation fraction of ITER-FEAT (∼0.75). Data from Monier-Garbet, et al. [34].

heating power. It has, of course, been already shown (Table I, Fig.4) that a reactor can accept energy confinement poorer than H-mode provided large radiation fractions can be avoided. Avoiding large radiation fractions appears to be the only reactor option, since present experimental data and theoretical understanding show that ITBs too are not likely to extrapolate favorably to a highly radiating reactor.

A. High SOL radiation with ITBs

Since an ITB is separated from the edge, it would seem possible that an ITB plasma could get good confinement despite high SOL radiation. A fully detached plasma can radiate much more power than a partially detached one, but the price paid is that the H-mode transport barrier at the edge is lost. Let us now explore if a fully detached ITB reactor is plausible.

The discussion in Appendix B shows that a detached plasma will have either a pedestal

that is little different from an L-mode edge, or an actual L-mode edge. Experiments on DIII-D, JET, and JT-60 find that MHD beta limits are very low for ITB plasmas with an L-mode edge. The plasma disrupts at $\beta_N \sim 2$ or below [57–60] - much lower than the values needed for a power reactor (or even for the proposed AT operation in ITER-FEAT). The association of pressure peaking and low β_N is confirmed by experiments [57, 61] and analysis [62] that show that plasmas with an H-mode edge (and thus broader pressure profiles) can attain a larger β_N. Ideal stability analysis also finds that wall stabilization causes little improvement in the beta limit of plasmas with highly peaked pressure profiles [62].

A reactor must have a high β_N along with good confinement. The best β_N from experiments with an L-mode edge is $\sim$ half that of the best plasmas with an H-mode edge.

Given the discouraging experimental results for ITB plasmas with an L-mode edge, one must conclude that reactor grade plasmas will require an H-mode edge, and hence fully detached plasmas are not a viable option even for ITB operations. Thus the severe limitations on the SOL radiative capacity that forced a large core radiation fraction for the standard H-mode, pertain even for an ITB operation. There is no escape from large core radiation fraction if the divertor/SOL region is not fundamentally redesigned.

B. High core radiation with ITBs - No Escape from High Radiation Trap

The next step in the further exploration of ITBs is to investigate whether such a plasma can remain reactor-relevant if its core is made highly radiating ($f_{Rad,Core} \sim 85\%$), instead of its SOL. Following the methodology employed for the H-mode reactors, we calculate the required confinement enhancement factor above the L-mode (we define L-mode confinement as the prediction of the ITER89P scaling law [64]) for a variety of advanced tokamak reactors with and without radiation. As in the H-mode analysis, we have subtracted the radiation power from the heating power to estimate the stored energy.

The required H89P factors for AT reactors EU-C, ARIES RS, and CREST are displayed in Table II. The difference between the second and third columns is striking - without subtracting radiation, the required confinement multipliers are rather modest and well within the range of experiment, but when the radiation is subtracted, the required confinement enhancements become extremely demanding. It is even more difficult to obtain such large H factors in an integrated discharge with high β_N, high bootstrap current fraction, and with

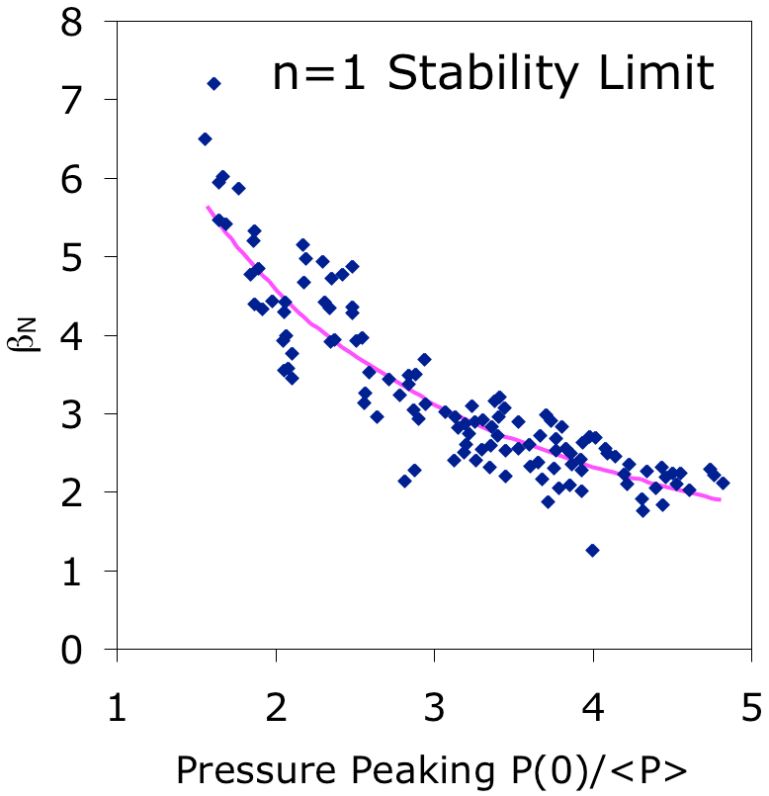

FIG. 6: Experimental DIII-D data and analysis showing that β_N strongly drops with pressure peaking for AT shots (even with wall stabilization). Data from Ferron, et al. [63].

reactor relevant ratio of ion to electron temperatures $T_i/T_e \sim 1$.

Device	**Heating Power P [MW]**	$\mathbf{H}_{89P}$ for AT Mode	$\mathbf{H}_{89P}$ Subtracting $P_{Rad,Core}$	β_N
ARIES-RS	515	2.1	4.6	4.8
CREST	691	1.6	4.5	5.5
EU-C	792	1.5	3.6	3.7

TABLE II: Requirements for the confinement enhancement above L-mode scaling for advanced tokamak reactor studies.

From the experimental results for H89P in advanced tokamak operation compiled by Sips [61] in the multi-machine ITPA database, we display a plot of H89P against T_i/T_e in Fig.7. For a burning plasma, it is well accepted that T_i/T_e will be close to unity, and possibly less. As noted by Sips, there is a trend toward lower H89P as T_i/T_e approaches unity. This may be because the stabilization of ion temperature gradient (ITG) modes is generally regarded

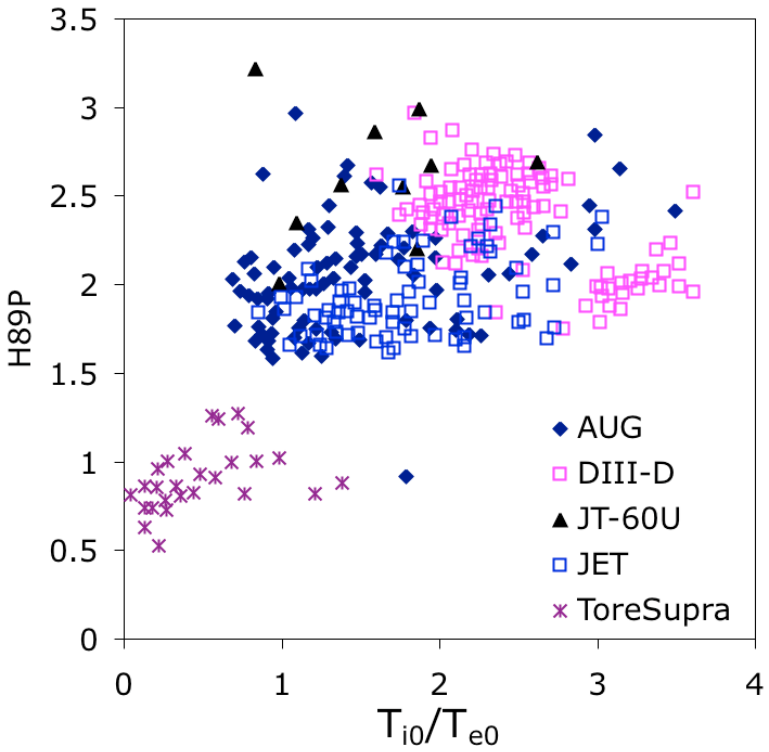

FIG. 7: Confinement enhancements over ITER89P L-mode scaling vs T_i/T_e. Confinement is no better than H-mode for reactor-relevant T_i/T_e =1. Data from Sips, et al. [61].

as the cause for ITB formation, and theory indicates that ITG stabilization is easier when $T_i/T_e > 1$.

The experimental results show that confinement with ITBs is, in most cases, not much better than H-mode (H89P $\sim$2) when $T_i/T_e \sim 1$. This, as we noted in Sec.III, is quite adequate without a large core radiation fraction, but with high core radiation fractions, considerably better confinement is demanded. The need for very high confinement enhancements above L-mode becomes worrisome when one considers that velocity shear is thought to be important in sustaining transport barriers, and a burning plasma has much less velocity shear than present experiments. This is true for both the intrinsic velocity shear, which is proportional to ρ^* (the thermal gyro radius normalized to the minor radius), as well as for the driven rotation shear [5].

Radiation removes the transport power which sustains the ITB. In Fig.8, the heating power per particle for the onset of an ITB is plotted versus $1/\rho^*$. For $\sim$ 80% radiation fraction, we see that the net reactor heating power is about an order of magnitude below the threshold indicated by experiments. Without radiation, the heating power is about a factor

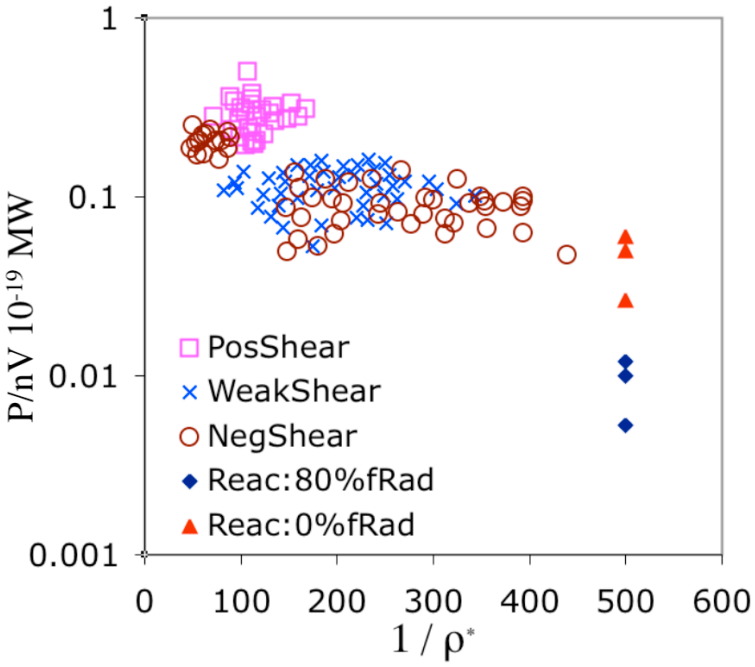

FIG. 8: Heating power per particle (in 10^{-19} MW) for the onset of an ITB verses $1/\rho^*$. ASDEX-U, DIII-D, JET, JT-60U, and TFTR data for the heating power per particle for ITB onset, from Connor, et al. [5].

of 2 below the threshold. Experiments can operate with heating power a factor of two below the threshold [65] (though the pressure profile may become more peaked, which is a concern for MHD beta). However, having to depend on ITB operation an order of magnitude below the apparent power threshold for ITB onset is very worrisome.

The possibility of radiating high powers in the core is analyzed in more detail in Appendix F. The main conclusions are: 1) There is experimental evidence that the confinement deteriorates even more rapidly with radiation inside the ITB than indicated by the formula of subtracting the radiation power from the L-mode scaling law; the confinement requirements for a highly radiating ITB reactor may be even more daunting than indicated in Table II, and 2) It seems impossible to radiate substantially outside the ITB (but still in the plasma in the core) for reactor relevant temperatures and for pressure and density profiles consistent with good MHD beta. Typically, about $\sim 90\%$ of the radiation is inside the ITB foot. These conclusions stem from taking profiles similar to those on the most relevant experimental discharges and scaling them up to reactor temperatures to compute the radiation profiles.

On extrapolating relevant experimental results, the high confinement requirements for

large radiation fractions in the core are found to be extremely demanding, realizing that a reactor must have profiles consistent with high beta and a high fraction of the current given by the bootstrap current. These extrapolations may be optimistic since the reactor will also suffer from greatly reduced velocity shear and will have $T_i/T_e \sim 1$.

When one adds to this to a) the extreme thermal instability that the ITB discharge is prone to at high radiation fraction (see Sec.V), and b) the possibility of core collapse from Helium build-up (see Sec.IV C), reactor operation with an ITB does not appear to provide a way out of the radiation trap imposed by the standard divertor (SD).

C. Helium build-up - Core radiation collapse

Even if it were somehow possible to obtain ITBs with high enough confinement, the plasma transport will be too low for adequate helium exhaust - the result will be a radiation collapse of the core inside the ITB. To analyze this situation, we build a model similar to that of Wade et al. [35]. Assuming temperature and electron and impurity density profiles pertinent to an ITB reactor (see Appendix F), the fusion heating and radiation power can be computed from known cross sections. The heat diffusivity χ, consistent with the profiles and the net heat fluxes, can then be derived. The source of helium from fusion can also be computed. To compute helium density, one needs appropriate transport coefficients. The first step in this direction is provided by the experimental findings [66] that the helium diffusivity in H-modes is roughly 0.7 times the total heat diffusivity, and the helium pinch is the same as the density pinch. We use these results in the region outside the ITB. For inside the ITB, we assume purely diffusive helium transport, motivated by the JT-60U [67] result that the helium diffusivity inside the ITB is determined to be between $0.2 - 1.0$ times the ion heat diffusivity (and the helium pinch in the ITB is assumed zero). The ion heat flux is about $\sim 70\%$ of the total heat flux. These results allow the helium density to be determined via a 1D transport analysis.

For a sufficiently low helium diffusivity, the helium in the core builds up until the radiation rate inside the ITB exceeds the decreasing fusion heating rate, and there is no solution. In practice, a core radiation collapse would occur. The maximum tolerable impurity peaking before the radiation collapse, naturally, depends on helium diffusivity. In Fig.9, the maximum impurity peaking is plotted versus helium diffusivity. For core radiation fractions

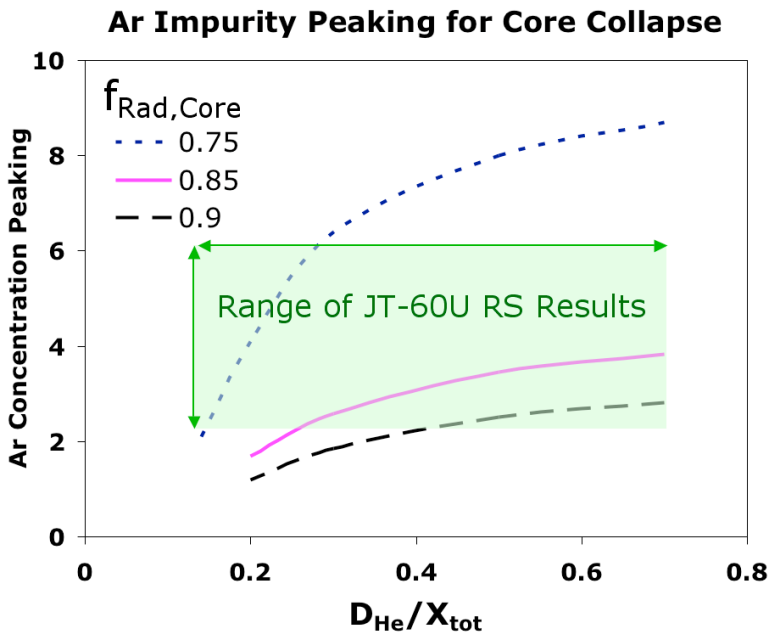

FIG. 9: Maximum tolerable impurity density (Ar) peaking verses helium diffusivity.

$f_{Rad,Core} \sim 85\%$, most of the existing experiments lie in the range of radiation collapse. For $f_{Rad,Core} \sim 70\%$, most of the data is outside the range for radiation collapse. On the basis of extrapolations of existing data, we conclude that at core radiation fractions $\sim 85\%$, there exists a substantial possibility of core collapse due to Helium buildup in ITB discharges.

V. THERMAL INSTABILITY IN A BURNING PLASMA WITH A HIGH RADIATION FRACTION

A unique feature of burning plasmas is that a high core radiation fraction $f_{Rad,Core}$ causes a strong thermal instability; this instability is not present in externally heated plasmas. The self-heating dynamics of such a plasma makes it prone to rapid swings in the power output. To examine the stability of the evolution equation

$$n\frac{dT}{dt} = -\frac{nT}{\tau_E} + P, \tag{5}$$

we use the temperature dependence of the heating power P(= fusion alpha power P_α + external power P_{ext} - radiation power P_{Rad}) and the confinement time τ_E. Empirical scaling laws give τ_E as a function of the heating power P. To write the confinement time as a function of the average plasma temperature, one invokes the relation $P\tau_E = nTV$, where the

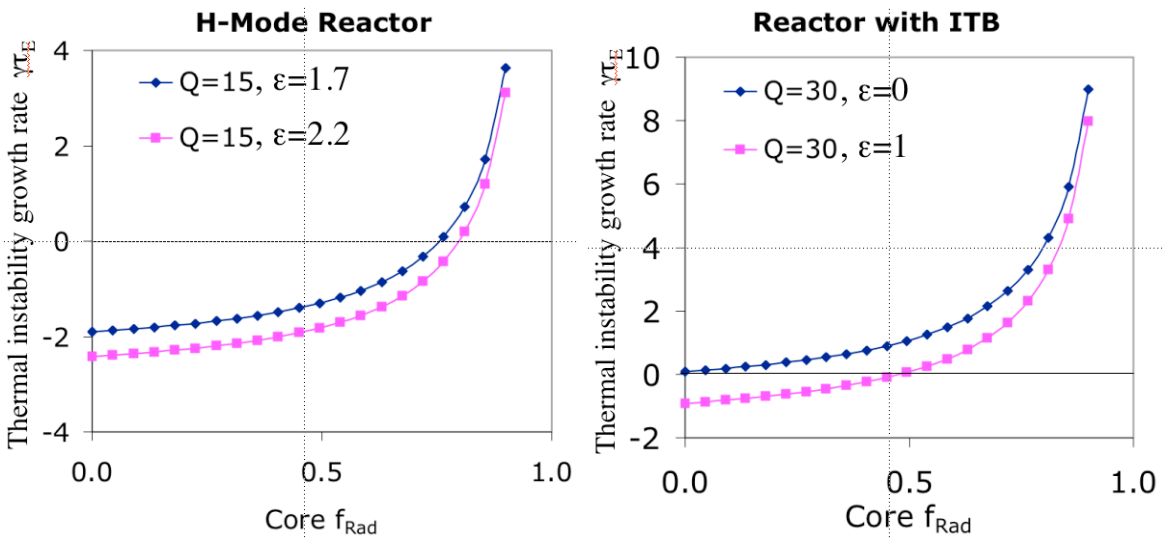

FIG. 10: Thermal instability growth rate $\gamma\tau_E$ verses core radiation fraction in a reactor with H-mode or one with ITB. The growth rate increases very rapidly beyond f_{Rad}=0.7.

volume $V = 4\pi Ra^2\kappa$, R, a, and κ are the major radius, the minor radius and the elongation, respectively. For the H-mode scaling law ITER98H(y,2), the power dependence of $\tau_E \sim P^{-0.69}$ translates to a temperature dependence of $\tau_E \sim T^{-\epsilon}$, with $\epsilon = 2.2$. Temperature perturbations also change the heating power. We presume for simplicity that the spatial dependence of the temperature profile stays the same (as in stiff core transport), and the whole profile changes multiplicatively. Then, in the vicinity of a given temperature, the heating power goes as $\sim T^{\alpha}$. Similarly, the radiation power changes as T^{ρ}. Temperature perturbations can be be shown to have a growth rate γ, which when normalized to the net energy confinement time τ_E, takes the form

$$\gamma\tau_E = \frac{1}{1 - f_{Rad,Core}} \left[\frac{\alpha}{1 + 5/Q} - \rho f_{Rad,Core} \right] - (\epsilon + 1) \tag{6}$$

where Q is the external plasma heating power (assumed constant in time) divided by the total fusion energy (including that of neutrons). For H-mode like profiles and the reactor temperature of EU-B, $\alpha = 1.06$, and $\rho = 0.18$ for Argon (we have found that Argon leads to the best thermal stability, so we take the impurity to be Argon in this section). The growth rates are plotted in Fig.10.

The thermal instability growth rate is an increasing function of the radiation fraction, and the normalized growth rate becomes singular as $f_{Rad,Core}$ approaches unity. This system is always stable if the fusion power is negligible (present experiments), or if there is no

radiation. ITER-FEAT with Q=10 and $f_{Rad,Core} \sim 40\%$ is stable. For Q = 15, similar to EU-B, the thermal instability threshold is 0.8, and at $f_{Rad,Core} = 0.85$, the calculated growth rate is $\sim 1/\tau_E$. The thermal instability growth rate is sensitive to the exponent in the energy confinement time. For example, with the other commonly used H-mode scaling law, ITERH98(y), the temperature dependence of τ_E is weaker, $\epsilon = 1.7$, and the thermal instability threshold for $Q = 15$ is $f_{Rad,Core} \sim 0.7$, and at $f_{Rad,Core} = 0.85$, $\gamma \sim 1.6/\tau_E$. Since it takes an impurity species a time $\sim \tau_E$ to penetrate into a plasma, stabilization possibilities by feedback on the impurity species are marginal.

For ITB discharges in JET the stored energy varies more strongly with input power than in the case of H-modes, implying a stronger thermal instability. With low central magnetic shear, the stored energy varies roughly as $P^{0.5}$, corresponding to $\epsilon = 1$ [68]. For JET reverse shear (RS) discharges the stored energy varies nearly linearly with the heating power $\sim P$, or $\epsilon \sim 0$ [69]. Advanced tokamak reactor studies (e.g. ARIES-RS, EU-C, and CREST) have $T \sim 16$ keV, which leads to $\epsilon = 1.27$ and $\gamma = 0.01$. The Q for these studies is ~ 30. The thermal instability growth rate (Fig.9) shows that, in the RS mode, the plasma is thermally unstable even without impurity radiation. With $f_{Rad,Core} \sim 0.85$, the growth rate $\gamma \sim 6/\tau_E$ is quite high implying a doubling time of ~ 2 sec for fusion power.

Advanced tokamak (AT) scenarios envisaged for ITER have much lower $Q \sim 5$, and are likely to be thermally stable, or only marginally unstable.

For ITB based reactors, the thermal instability is severe for the relevant range of $f_{Rad,Core}$. It is not possible to control such a virulent instability using feedback on the impurity puffing or fueling - these signals do not propagate into the core quickly enough. Only feedback on the external heating power might be fast enough, but this becomes progressively less robust at high Q, since the control signal has a small dynamic range. By increasing the power capacity of the divertor by merely a factor of ∼2-3, it is possible to stabilize the thermal instability, or at least slow its growth time to values longer than the confinement time so that impurity puffing or fueling can be used for feedback - these controls have a much larger dynamic range which makes them more robust. The new X-divertor (XD) proposed and described in Sec.VI increases the divertor power capacity to this range.

In a plasma with $\sim 95\%$ radiation, a small perturbation in fusion power will lead to a much larger change in the net power $(P_\alpha - P_{Rad})$ onto the divertor plate since the radiation does not increase commensurately with perturbations. For an ITB reactor with a high

radiation fraction, the doubling time of power on the plate would be a small fraction of a second. For a divertor plate close to the engineering limit, a short transient could cause damage requiring replacement (months of downtime). Thus, a crucial requirement for such a reactor is to demonstrate very effective stabilization of the thermal instability under all perturbing conditions that affect heating and radiation balance. Such perturbations could be: 1) routine and expected such as pellet injection and ELMs, or 2) sporadic occurrences like flakes of wall material falling into the plasma, and 3) off-normal events such as equipment transients and failures.

In principle such swings can perhaps be detected and feedback stabilized. The swing control, however, can become much more difficult as the ratio of the heating to the fusion power becomes lower (i.e. Q becomes higher, as it must in an attractive reactor). Thus if ITER-FEAT were to demonstrate the physics performance necessary for a power reactor, it must access and explore this thermally unstable range, and also demonstrate the feasibility of a robust scheme for feedback stabilization. However, will not have an H-mode at $f_{Rad}> 60\%$ ITER-FEAT, and cannot access and study strong alpha heating and core thermal instability - precisely the regimes critically relevant to an SD reactor.

There are other serious physics consequences of the core thermal instability. Because of its tendency to induce large power swings into the SOL, any modest drop in input power to a highly radiating SOL may cause an SOL radiation collapse. This, in turn, will cause a drop in core confinement, leading to a further loss of fusion power. The system may not recover from this vicious cycle. The thermal instability (caused by a high radiation fraction in the core - a necessity for an SD reactor) and its consequences should give us pause. A highly thermally unstable core plasma coupled to a highly radiating SOL is a novel complex physical system with much potential for disruption and hence questionable practicality, especially in a radioactive setting subject to strong regulations.

It is, therefore, highly desirable and perhaps mandatory to avoid operation of a reactor in a highly thermally unstable plasma regime. For this to work, the core radiation fraction required to save the divertor must fall below the threshold for thermal instability or at least fall enough that the thermal instability becomes weak. What we need, then, is to design and test divertors that can handle significantly more power than the standard divertors used on current and proposed machines. In Sec.VI, we will describe just such a class of divertors with large flux expansion that enables them to handle much higher heat fluxes.

VI. NEW DIVERTORS - INCREASED HEAT FLUX CAPABILITY

In the preceding sections we have shown that the divertor is the key element in the thermal architecture of a fusion reactor, and that the limited heat-rating of the standard divertors (SD) makes it extremely difficult to find a reactor-relevant operating regime. In Sec.IV we also demonstrated that the XD devices, with new X-Divertors whose heat-handling capacity is much higher than SD devices, can relatively easily fulfill the confinement and other demands for a high power fusion reactor. This section is devoted to a detailed discussion of the concept and feasibility of this new X-divertor.

The new divertors [22, 23] will be able to withstand roughly 3 times more power as compared to the standard, optimized ITER-like divertors [13]. The high power rating is brought about by vastly increasing the plasma-wetted area through small but carefully designed changes in the poloidal magnetic field in the divertor region.

The obvious first step is to try to increase the plasma-wetted area on the divertor plate by tilting the plates to decrease the poloidal strike angle. This is a standard optimization practice and the power limits on the standard divertors quoted in this paper had already been subjected to tilt optimization. However, for tilt angles less than about 25 degrees, this technique yields little improvement [29] or no improvement [30] in power handling. The novel divertors can and do use the standard optimizing methods, but the main source of their large gain is due to a fundamental change in the magnetic geometry of the divertor region. The main results from [22, 23] are summarized here.

The basic idea behind the new X-divertors (XD, Fig.11) is to flare the field lines downstream from the main plasma X-point. As shown in Fig.11, while field lines converge as they move downstream from the X-point in a standard divertor (SD), they can be made to diverge by creating another X-point near the divertor plate. This extra downstream X-point can be easily created with an extra pair of poloidal coils (dipole: with opposing currents). Each divertor leg (inside and outside) needs such a pair of coils. For a reactor, this would entail linked coils. To avoid this unacceptable situation, the axisymmetric coils can be replaced with smaller modular coils that produce the same axisymmetric field components. Their non-axisymmetric ripple in the plasma has been shown to be small ($< 0.3\%$) for this configuration. In this respect, these X-divertors (XD) are completely different from the old bundle divertors which created a large ripple in the main plasma. Since one needs to cancel

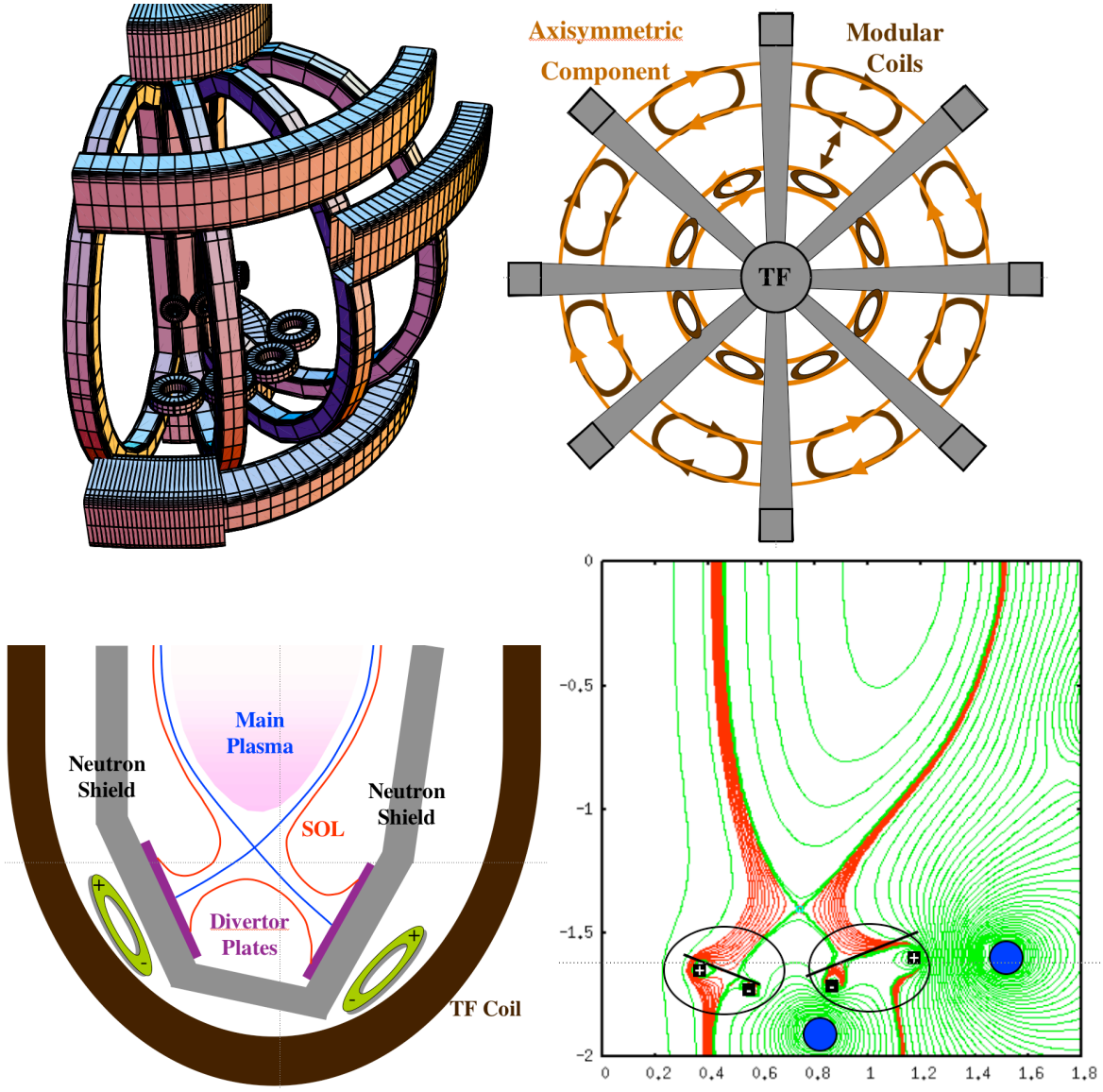

FIG. 11: Top left: Modular X-divertor (XD) coil loops (which can be rectangular). Note that the plasma *does not go through the loops* - the loops are behind the divertor plates (these are not bundle divertors). Top right: The axi-symmetric component of the currents in the loops is equivalent to the axisymmetric poloidal coils (+ and −) with opposite currents. Only 8 TF coils are shown in this top view for clarity. Bottom left: Side view. Modular coils are behind neutron shield. Bottom right: Flux expansion (see encircled areas) in NSTX MHD equilibrium.

only the small poloidal field at the new X-point, the corresponding coil currents are small. However, the gain in the plasma wetted area can be very large (5 or more), as shown in Figs.11-12 and in Table II. The reduction in poloidal field also increases the line length ∼2-3

times, which will better isolate the plasma from divertor plate in the parallel direction. Impurity entrainment should be considerably enhanced, leading to better radiation capability, and lower impurities in the main plasma. Further, since the line flaring needs to be done only near the extra coils, the effects on the distant main plasma are small. An additional advantage is that it is easier to attain main plasma configurations of high triangularity (even inside indentation), high elongation, and high or low poloidal beta. Such configurations have very beneficial MHD implications.

The extra X-divertor (XD) coils could possibly be accommodated in an existing machine, or in a reactor with a modest increase in the complexity of the magnetic design and a very small or no increase in toroidal field volume. Although a design with the modular coils in the removable ITER divertor cassette is magnetically feasible (see Fig.11), practical engineering problems will probably prevent any such retrofit for ITER. However, this "conceptual design" exercise demonstrates the feasibility of using modular copper coils behind less shielding than superconducting coils for a reactor. Alternatively, their location can be behind the blanket and shield so that superconducting coils may be used, as in the CREST design. In summary, the small modular coils can be reactor-relevant, their positive impact on divertor performance can be large, while their negative impact on the main plasma (ripple) can be very small.

Device	**Divertor**	Flux expansion	L_{XT} (X to Target)	Ratio L_{XT}/L_{XM}
NSTX	Standard (SD)	2.3	5.3 m	0.29
	New X-div (XD)	20.4	6.9 m	0.32
ITER	Standard (SD)	4.3	23 m	0.45
	New X-div (XD)	22.7	65 m	1.12
CREST	Standard (SD)	3.3	37 m	0.74
	New X-div (XD)	23	75 m	1.19

TABLE III: SOL field line parameters of 3 equilibria obtained with FBEQ [32].

The extra X-points created by the modular coils lead to flux expansion by a factor of five or more, and an increase in SOL field line length (from the x point to the plate) by a factor of 2 to 3. These are shown in Table III for different machines.

The five-fold flux expansion increases the divertor power handling capability, and thus

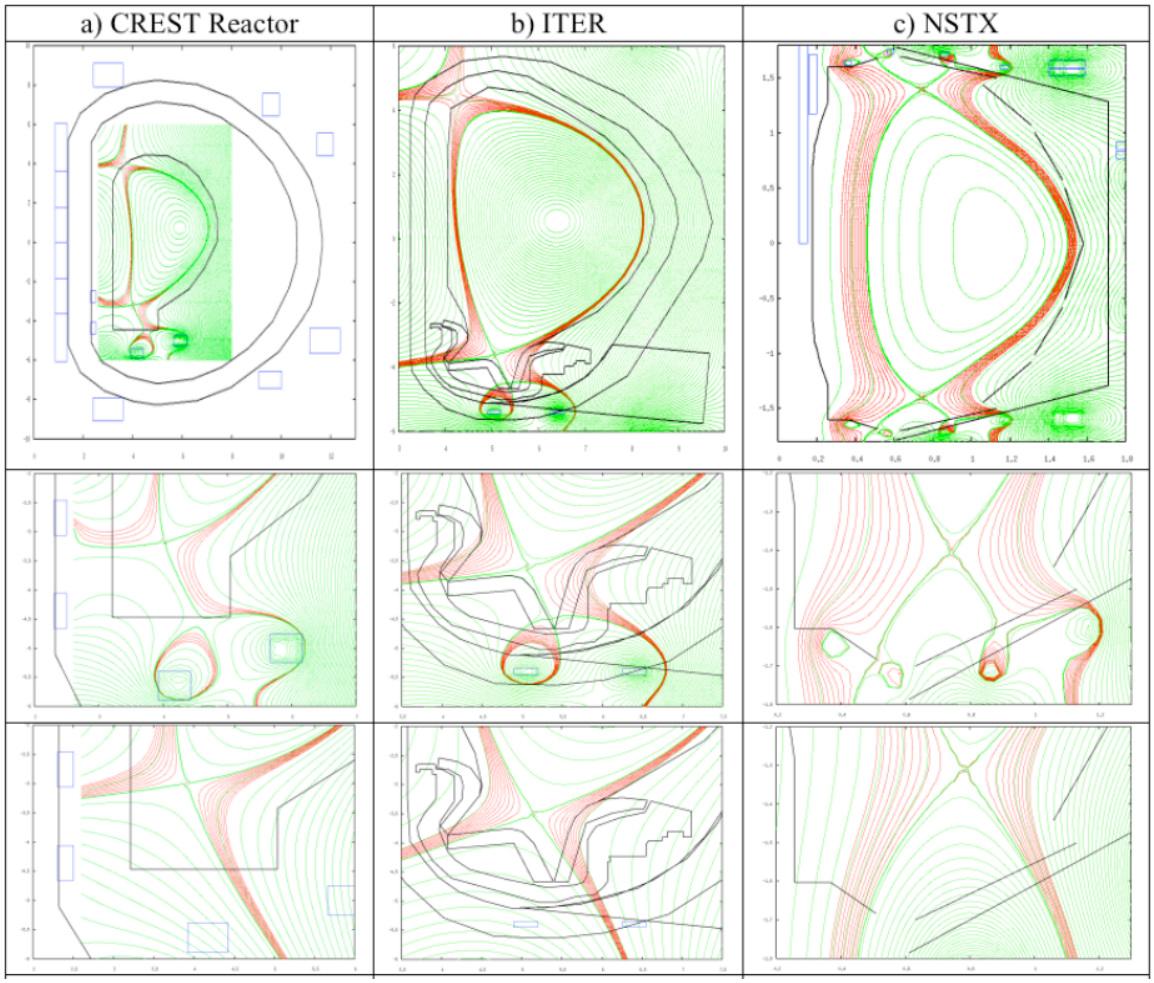

FIG. 12: New X-divertor (XD) equilibria for Left: CREST Reactor, Middle: ITER, and Right: NSTX. In each column, the second and third rows show the large flux expansion near the divertor plate when the new small coils are turned on and off respectively. For CREST and ITER, the coils are behind neutron shield. For ITER, coils can be designed to be inside divertor cassettes.

lowers the fraction of power that must be radiated in the core or the SOL. The new X-divertor (XD) brings the core radiation fractions in the range of present experiments and ITER-FEAT if we assume that the radiation in the new X-divertor (XD) is roughly the same as the ITER-FEAT value (a conservative assumption), given the improved impurity entrainment. This, as we have argued above, is the key to overcoming the major roadblock in the march to the higher power fusion reactors.

The core radiation fraction depends on the amount of power which can be radiated in the SOL. For ITER parameters with 100 MW of input power, roughly 60 MW is radiated

and 40 MW falls on the plate. We argued in Appendix A that the impurity radiation in the SOL is roughly independent of the line length. Therefore, we estimate that the total SOL radiation in the new X-divertor (avoiding detachment) will be about the same. It is possible that the increase in the line length will increase the radiation from neutrals, but we will not assume that here. If the power handling capacity of the plate could be increased to 200 MW (due to flux expansion by a factor of 5), the total power into the SOL could be increased to 260 MW. In adddition, increasing the line length L can slightly increases the SOL width as $L^{2/9}$ [27]. If the cross field thermal diffusion stays the same, the SOL width is increased by $\sim 20\%$, so the total power into the the SOL could be increased to roughly 300MW. Thus, we estimate that the new X-divertor (XD) geometry increases the SOL power by a factor of ~ 3 beyond the estimates given by Kukushkin [29].

Because of this, the core confinement requirements on the reactor plasma are substantially reduced - to a range which is comfortably within the present operating experience. For an H-mode reactor like EU-B, confinement could be at a level of about 85 percent of the nominal H-mode level. This is almost in the range of experiments with type III ELMs, which are estimated to give acceptable transient heat fluxes for a reactor [29, 34]. For AT based reactors such as EU-C and ARIES-RS, the confinement need be only slightly better than H-mode- within the range of so-called hybrid discharges with $H_H \sim 1.2$.

Furthermore, the thermal instability for EU-B would be avoided. For the ITB reactors, the thermal instability time would be slower than the confinement time, so feedback on the core impurity level should suffice. Also, core radiation fractions would be brought down to a level where Helium build-up and radiation collapse is very unlikely.

VII. CONCLUSIONS

We find that the standard divertor SD (used in current and proposed machines), with its highly limited heat-handling capability, emerges as an unacceptably weak link in the chain leading to a dependable and economic power reactor. The low heat rating of SD implies an extremely high radiation fraction in the plasma, which in turn, has devastating effects on the core confinement and stability of a burning plasma. In the main text and in the appendices, we have shown that present experimental experience implies that a reactor employing the standard divertor (SD) cannot have acceptable confinement and β at the same time, and will

have a high risk of thermal instability and disruptions. These conclusions apply to operation with ITBs as well as H-modes.

The most spectacular but negative consequence of high f_{Rad} is the termination of the experimentally demonstrated robust and consistent favorable scaling (towards self-sustained thermonuclear reactions) with size, magnetic field and power level. The favorable scaling can be restored by increasing the heat handling capability of the divertor (by modifying its magnetic geometry); this will allow us to extrapolate the present experiments to reactors.

We have described such a divertor (X-divertor, or XD) whose capacity is increased ($\sim$ factor of 5) via the flaring of field lines. By reducing the radiation fraction to manageable levels, the new X-divertor could vastly reduce the requirements on core confinement. In fact, confinement times less than the ones predicted by H-mode scaling laws can suffice for some reactor designs. The most important consequences of the reduced radiation fraction is that the robust favorable scaling with size and power level (that had been replaced by an adverse scaling with power level for the SD machines with high radiation fraction) is restored for high power machines. Within the class of machines using the new X-divertor, one could, then, readily and confidently extrapolate the results obtained on relatively low power burning plamas to reactors. It has been shown in the main text that this relatively easy extrapolation to a reactor is denied to burning plasma machines with the SD because the lower power machines cannot even mimic the relevant regimes required for a reactor with a standard divertor.

Since the divertor part of the magnetic bottle assumes immense and critical importance as one approaches reactor power levels (it controls the behavior of the plasma core), much attention must be paid to the design, construction and testing of divertors with heat capacity much larger than the standard divertor . The X-divertor configuration presented in this paper can serve as a representative of this new class. The new X-divertor also opens the possibility of an attractive route to fusion through the following possible steps : 1) Test the new X-divertor by modifying one or more of the current machines, 2) build a modest cost and size copper based burning plasma experiment, but with the new X-divertor. We have found nothing that will prevent this experiment from laying the groundwork for a Component Test Facility (CTF), and demonstrating the crucial physics for a credible fusion reactor. In fact, both the power and Q of such a device can be raised by simply making it larger (relying on the most dependable trend in past 30 years of fusion research), 3) build

a CTF. It is possible that (2) and (3) could be combined in a single venture, and finally 4) design a demonstration fusion reactor (DEMO) by simply making the machine bigger and more powerful.

VIII. ACKNOWLEDGMENTS

We gratefully acknowledge help from J. Wiley and M. Pekker. This work was supported by ICC Grants from US DOE.

---

* Email:pvalanju@mail.utexas.edu

[1] G. Marbach, I. Cook, and D. Maisonnier, Fusion Eng. Des. **63-64**, 1 (2002).

[2] F. Najmabadi and the ARIES Team, Fusion Eng. Des. **38**, 3 (1997).

[3] K. Okano, Y. Asaoka, T. Yoshida, M. Furuya, K. Tomabechi, Y. Ogawa, N. Sekimura, R. Hiwatari, T. Yamamoto, T. Ishikawa, et al., Nucl. Fusion **40**, 635 (2000).

[4] D. J. Campbell, Phys. Plasmas **8**, 2041 (2001).

[5] J. Connor, T. Fukuda, X. Garbet, C. Gormezano, V. Mukhovatov, M. Wakatani, the ITB Database Groupa, the ITPA Topical Group on Transport, and I. B. Physics, Nucl. Fusion **44**, R1 (2004).

[6] E. J. Synakowski, Plasma Phys. Control. Fusion **40**, 581 (1998).

[7] Editors, Nuclear Fusion **39**, 2137 (1999).

[8] I. Cook, N. Taylor, D. Ward, L. Baker, and T. Hender, Tech. Rep. 521, UKEA FUS, Euratom/UKEA Fusion Association (2005).

[9] ASDEX, see http://www.ipp.mpg.de/eng/for/projekte/asdex/for_proj_asdex.html for details.

[10] DIII-D, see http://fusion.gat.com/diii-d/ for details.

[11] JET, see http://www.jet.efda.org/ for details.

[12] JT-60U, see http://www-jt60.naka.jaea.go.jp/HOME.html for details.

[13] A. S. Kukushkin, H. D. Pacher, G. Federici, G. Janeschitz, A. Loarte, and G. W. Pacher, Fusion Eng. Des. **65**, 355 (2003).

[14] V. Mukhovatov, M. Shimada, A. N. Chudnovskiy, A. E. Costley, Y. Gribov, G. Federici,

O. Kardaun, A. S. Kukushkin, A. Polevoi, V. D. Pustovitov, et al., Plasma Phys. Control. Fusion **45**, A235 (2003).

[15] A. S. Kukushkin, H. D. Pacher, G. W. Pacher, G. Janeschitz, D. Coster, A. Loarte, and D. Reiter, Nucl. Fusion **43**, 716 (2003).

[16] I. Cook, N. P. Taylor, and D. J. Ward, in *Proceedings of the Symposium on Fusion Engineering* (San Diego, 2003).

[17] C. S. Pitcher and P. C. Stangeby, Plasma Phys. Control. Fusion **39**, 779 (1997).

[18] M. Narula, A. Ying, and M. A. Abdou, Fusion Science and Technology **47**, 564 (2005).

[19] M. Abdou, N. Morley, T. Sketchley, R. Woolley, J. Burris, R. Kaita, P. Fogarty, H. Huang, X.Lao, M. Narula, et al., Fusion Engineering and Design **72**, 35 (2004).

[20] X. Zhou and M. S. Tillack, Tech. Rep. UCSD-ENG-079, University of California, San Diego (1998).

[21] M. T. Kotschenreuther, L. Zheng, and T. Rognlien, p. ICP04 (2002).

[22] M. T. Kotschenreuther, P. M. Valanju, and S. M. Mahajan, in *Proceedings of the 20th International Conference on Fusion Energy* (Vilamoura Portugal, 2004).

[23] M. T. Kotschenreuther, P. M. Valanju, and S. M. Mahajan (2004), submitted to Fusion Engineering Design.

[24] M. A. Abdou, Fusion Engineering and Design **27**, 111 (1995).

[25] P. Norajitra, R. Giniyatulin, T. Ihli, G. Janeschitz, P. Karditsas, W. Krauss, R. Kruessmann, V. Kuznetsov, D. Maisonnier, I. Mazul, et al., in *IAEA FT/P7-13* (2004).

[26] S. J. Zinkle, National Academy of Engineering publications **28** (1998).

[27] P. C. Stangeby, *The Plasma Boundary of Magnetic Fusion Devices* (IOP Publishing Ltd, 2000).

[28] W. Fundamenski, S. Sipil, and J.-E. contributors, Nucl. Fusion **44**, 20 (2004).

[29] A. S. Kukushkin, H. D. Pacher, G. Janeschitz, A. Loarteb, D. Costerc, and D. Reiterd, in *Proceedings of the 28th EPS conference on Controlled Fusion and Plasma Physicsth EPS Conference on Controlled Fusion and Plasma Physics* (Funchal, 2001).

[30] A. S. Kukushkin, H. D. Pachera, G. Janeschitz, D. Costerb, D. Reiterc, and R. Schneider, in *Proceedings of the 26th EPS Conference on Controlled Fusion and Plasma Physics* (Maastricht, 1999), vol. 231, pp. 1545–1548.

[31] A. Kallenbach, N. Asakura, A. K. A. Kirk, M. Mahdavi, D. Mossessian, and G. Porter, J.

Nucl. Mater. **337-339**, 381 (2005).

[32] D. Strickler, in *Proceedings, IEEE Thirteenth Symposium on Fusion Engineering* (1990), p. 898.

[33] ITER, in *ITER-FEAT Outline Design Report ITER meeting* (Tokyo, 2000).

[34] P. Monier-Garbet, P. Andrew, P. Belo, G. Bonheure, Y. Corre, K. Crombe, P. Dumortier, T. Eich, R. Felton, J. Harling, et al., in *Proceedings of the 20th International Conference on Fusion Energy* (Vilamoura, Portugal, 2004), vol. EX/P1-2.

[35] M. R. Wade, W. P. West, R. D. Wood, S. L. Allen, J. A. Boedo, N. H. Brooks, M. E. Fenstermacher, D. N. Hill, J. T. Hogan, R. C. Isler, et al., J. Nucl. Mater. **266-269**, 44 (1999).

[36] A. W. Leonard, M. A. Mahdavi, S. L. Allen, N. H. Brooks, M. E. Fenstermacher, D. N. Hill, C. J. Lasnier, R. Maingi, G. D. Porter, T. W. Petrie, et al., Phys. Rev. Lett. **78**, 4769 (1997).

[37] C. Angioni, A. G. Peeters, G. V. Pereverzev, F. Ryter, G. Tardini, and ASDEX-U, Phys. Rev. Lett. **90**, 205003 (2003).

[38] M. Greenwald, J. L. Terry, S. M. Wolfe, S. Ejima, M. G. Bell, S. M. Kaye, and G. H. Neilson, Nuclear Fusion **28**, 2199 (1988).

[39] H. Weisen, A. Zabolotsky, C. Angioni, I. Furno, X. Garbet, C. Giroud, H. Leggate, P. Mantica, D. Mazon, J. Weiland, et al., Nuclear Fusion **45**, L1 (2005).

[40] G. F. Matthews, S. Allen, N. Asakura, J. Goetz, H. Guo, A. Kallenbach, B. Lipschultz, K. McCormick, M. Stamp, U. Samm, et al., Nucl. Fusion **39**, 19 (1999).

[41] M. E. Fenstermacher, J. Boedo, R. C. Isler, A. W. Leonard, G. D. Porter, D. G. Whyte, R. D. Wood, S. L. Allen, N. H. Brooks, R. Colchin, et al., Plasma Phys. Control. Fusion **41**, A345 (1999).

[42] D. P. Coster, in *Proceedings of 10th International Toki Conference on Plasma Physics and Controlled Nuclear Fusion* (Toki-city Japan, 2000), pp. 1–5.

[43] A. S. Kukushkin, H. Pacher, G. Janeschitz, A. Loarte, D. Coster, G. Matthews, D. Reiter, R. Schneider, and V. Zhogolev, Nucl. Fusion **42**, 187 (2002).

[44] K. Borrass, A. Loarte, C. Maggi, V. Mertens, P. Monier, R. Monk, J. Ongena, J. Rapp, G. Saibene, R. Sartori, et al., Nucl. Fusion **44**, 752 (2004).

[45] J. Pamela, J. Ongena, and J. E. Contributors, Nucl. Fusion **45**, 563 (2005).

[46] J. Rapp, A. Huber, L. C. Ingesson, S. Jachmich, G. F. Matthews, V. Philipps, R. Pitts, and

C. to the EFDA-JET work programme, J. Nucl. Mater. **313-316**, 524 (2002).

[47] M. T. Kotschenreuther, W. Dorland, Q. P. Liu, G. W. Hammett, M. A. Beer, S. A. Smith, A. Bondeson, and S. C. Cowley, in *Proceedings of the 16th IAEA Fusion Energy Conference* (Montreal, Canada, 1996).

[48] R. E. Waltz, G. M. Staebler, W. Dorland, G. W. Hammett, M. Kotschenreuther, , and J. A. Konings, Phys. Plasmas **4**, 2482 (1997).

[49] J. E. Kinsey, in *Proceedings of the 19th International Conference on Fusion Energy* (Vilamoura Lyon, 2002).

[50] M. Becoulet, G. Huysmans, Y. Sarazin, X. Garbet, P. Ghendrih, F. Rimini, G. Huysmans, Y. Sarazin, X. Garbet, P. Ghendrih, et al., Plasma Phys. Control. Fusion pp. A93–A113 (2003).

[51] R. Sartori, G. Saibene, M. Becoulet, P. J. Lomas, A. Loarte, D. J. Campbell, Y. Andrew, R. Budny, M. N. A. Beurskens, A. Kallenbach, et al., Plasma Phys. Control. Fusion **44**, 1801 (2002).

[52] R. Sartori, G. Saibene, L. D. Horton, M. Becoulet, R. Budny, D. Borba, A. . Chankin, G. D. Conway, G. Cordey, D. McDonald, et al., Plasma Phys. Control. Fusion **46**, 723 (2004).

[53] S. Higashijima, N. Asakura, H. Kubo, Y. Miura, T. Nakano, S. Konoshima, K. Itami, S. Sakurai, H. Takenaga, H. Tamai, et al., J. Nucl. Mater. **313-316**, 1123 (2003).

[54] G. Maddison, M. Brix, R. Budny, M. Charlet, and I. Coffey, Nucl. Fusion **43**, 49 (2003).

[55] D. Kalupin, P. Dumortier, A. Messiaen, J. Ongena, B. Unterberg, R. Weynants, R. Jaspers, R. Koslowski, G. Mank, and G. V. Wassenhove, in *Proceedings of the 27th EPS Conference on Controlled Fusion and Plasma Physics* (Budapest, 2000), vol. 24B, pp. 1417–1420.

[56] H. R. Koslowski, G. Fuchsa, R. Jaspersb, A. Kramer-Fleckena, A. Messiaen, , J. Ongenac, , J. Rappa, F.C.Schullerb, et al., Nucl. Fusion **40**, 821 (2000).

[57] E. A. Lazarus, G. A. Navratil, C. M. Greenfield, E. J. Strait, M. E. Austin, K. H. Burrell, T. A. Casper, D. R. Baker, J. C. DeBoo, E. J. Doyle, et al., Phys. Rev. Lett. **77**, 2714 (1996).

[58] A. Sips and the JET Team, Nucl. Fusion **41**, 1559 (2001).

[59] T. Fujita, Y. Kamada, S. Ishida, Y. Neyatani, T. Oikawa, S. Ide, S. Takeji, Y. Koide, A. Isayama, T. Fukuda, et al., Nucl. Fus. **39**, 1627 (1999).

[60] S. Takeji, S. Tokuda, T. Fujita, T. Suzuki, A. Isayama, S. Ide, Y. Ishii, Y. Kamada, Y. Koide, T. Matsumoto, et al., Nucl. Fusion **42**, 5 (2002).

[61] A. C. C. Sips, E. J. Doyle, C. Gormezano, Y. Baranov, E. Barbato, R. Budny, P. Gohil, F. Imbeaux, E. Joffrin, T. Fujita, et al., in *Proceedings of the 20th International Conference on Fusion Energy* (Vilamoura, Portugal, 2004), pp. 1–8.

[62] A. D. Turnbull, T. S. Taylor, M. S. Chu, R. L. Miller, and Y. R. Lin-Liu, Nucl. Fusion **38**, 1467 (1998).

[63] J. R. Ferron, T. A. Casper, E. J. Doyle, A. Garofalo, P. Gohil, C. Greenfield, A. Hyatt, R. J. Jayakumar, C. Kessel, T. C. Luce, et al., in *Proceedings of the 20th International Conference on Fusion Energy* (Vilamoura, Portugal, 2004).

[64] P. N. Yushmanov, T. Takizuka, K. S. Reidel, O. J. W. F. Kardaun, J. G. Cordey, S. M. Kaye, and D. E. Post, Nuclear Fusion **30**, 1999 (1990).

[65] Y. F. Baranov, C. Bourdelle, T. Bolzonella, M. D. Baar, C. D. Challis, C. Giroud, N. C. Hawkes, E. Joffrin, and V. P. Ridolfini, Plasma Phys. Control. Fusion **47**, 975 (2005).

[66] M. R. Wade, T. C. Luce, and C. C. Petty, Phys. Rev. Lett. **79**, 419 (1997).

[67] H. Takenaga, Nucl. Fusion **45** (2003).

[68] P. Buratti and the JET Team, in *Proceedings of the 18th International Conference on Fusion Energy* (Sorrento Italy, 2000).

[69] C. D. Challis, X. Litaudon, G. Tresset, Y. F. Baranov, A. Becoulet, C. Giroud, N. C. Hawkes, D. F.Howell, E. Joffrin, P. J. Lomas, et al., Plasma Phys. Control. Fusion **44**, 1031 (2002).

[70] V. Mertens, K. Borrass, J. Gafert, M. Laux, J. Schweinzer, and A. U. Team, Nucl. Fusion **40**, 1836 (2000).

[71] R. Maingi, M. A. Mahdavi, T. W. Petrie, L. R. Baylor, T. C. Jernigan, R. J. L. Haye, A. W. Hyatt, M. R. Wade, J. G. Watkins, and D. G. Whyte, J. Nucl. Mater. **266-269**, 598 (1999).

[72] A. V. Chankin, K. Itami, and N. Asakura, Plasma Phys. Control. Fusion **44**, A399 (2002).

[73] G. M. McCracken, R. D. Monk, A. Meigs, L. Horton, L. C. Ingesson, J. Lingeretat, G. F. Matthews, M. G. OMullane, R. Prentice, M. F. Stamp, et al., J. Nucl. Mater. **266-269**, 37 (1999).

[74] W. Suttrop, V. Mertens, H. Murmann, J. Neuhauser, J. Schweinzer, and A.-U. Team, J. Nucl. Mater. **266-269**, 118 (1999).

[75] M. A. Mahdavi, T. H. Osborne, A. W. Leonard, M. S. Chu, E. J. Doyle, M. E. Fenstermacher, G. R. McKee, G. M. Staebler, T. W. Petrie, M. R. Wade, et al., Nucl. Fusion **42**, 52 (2002).

[76] T. W. Petrie, S. L. Allen, T. N. Carlstrom, D. N. Hill, R. Maingi, D. Nilson, M. Brown, D. A.

Buchenauer, T. E. Evans, M. E. Fenstermacher, et al., J. Nucl. Mater. **241-243**, 639 (1997).

[77] T. W. Petrie, in *Proceedings of the 28th EPS conference on Controlled Fusion and Plasma Physics* (Madiera, Portugal, 2001).

[78] S. Konoshima, H. Tamai, Y. Miura, S. Higashijima, H. Kubo, S. Sakurai, K. Shimizu, T. Takizuka, Y. Koide, T. Hatae, et al., J. Nucl. Mater. **313–316**, 888 (2003).

[79] A. Loarte, R. D. Monk, J. R. Martin-solis, D. J. Campbell, A. V. Chankin, S. Clement, S. J. Davies, J. Ehrenberg, S. K. Erents, and H. Y. Guo, Nucl. Fusion **38**, 331 (1998).

[80] J. Kinsey, G. Bateman, T. Onjun, A. Kritz, A. Pankin, G. Staebler, and R. Waltz, Nucl. Fusion **43**, 1845 (2003).

[81] J. W. Hughes, D. A. Mossessian, A. E. Hubbard, B. LaBombard, and E. S. Marmar, Phys. Plasmas **9**, 3019 (2002).

[82] A. E. Hubbard, A. E. Hubbard, B. Lipschultz, D. Mossessian, R. L. Boivin, J. A. Goetz, R. S. Granetz, M. Greenwald, I. H. Hutchinson, D. J. J. Irby, et al., in *Proceedings of the 26th EPS Conference on Controlled Fusion and Plasma Physics* (Maastricht, 1999), pp. 13–16.

[83] F. Ryter, A. Stabler, and G. Tardini, Fusion Science and Technology **44**, 618 (2003).

[84] T. Onjun, A. H. Kritz, G. Bateman, V. Parail, H. Wilson, J. Lonnoroth, G. Huysmans, and A. Denestrovskij, Physics of Plasmas **11**, 1469 (2004).

[85] Y. Kamada, H. Takenaga, H. Urano, T. Takizuka, T. Hatae, and Y. Miura, in *IAEA-CN-94 / EX / P2-04* (2002).

[86] P. Snyder (2006), private communications.

[87] M. Kotschenreuther, W. Dorland, M. A. Beer, and G. W. Hammett, Phys. Plasmas **2**, 2381 (1995).

[88] M. E. Puiatti, M. Mattioli, G. Telesca, M. Valisa, I. Coffey, P. Dumortier, C. Giroud, L. C. Ingesson, K. D. Lawson, G. Maddison, et al., Plasma Phys. Control. Fusion **44**, 1863 (2002).

[89] H. Kubo, S. Sakurai, S. Higashijima, H. Takenaga, K. Itami, S. Konoshima, T. Nakano, Y. Koide, N. Asakura, K. Shimizu, et al., J. Nucl. Mater. **313-316**, 1197 (2003).

[90] H. Takenaga, N. Asakura, H. Kubo, S. Higashijima, S. Konoshima, T. Nakano, N. Oyama, G. D. Porter, T. D. Rognlien, M. E. Rensink, et al., Nucl. Fusion **45** (2005).

[91] R. Dux, C. Giroud, K. Zastrow, and J. E. contributors, Nucl. Fusion **44**, 260 (2004).

[92] S. P. Hirshman and J. C. Whitson, Phys. Fluids **26**, 3553 (1983).

[93] NCSX, see `http://ncsx.pppl.gov//index.html` for details.

APPENDIX A: DIVERTOR RADIATION WITH CONVECTION

The widely used two-point model [27] is based on a one-dimensional model for the divertor temperature along a field line, where Spitzer themal conduction is responsible for parallel heat tranport. For highly radiating divertors, convection is also very important [36]. With convection, the energy transport equation along a field line in the SOL is [36]

$$\frac{d}{dl}\left[\kappa T^{5/2}\frac{d}{dl}T + nv\left(5T + \frac{1}{2}mv^2\right)\right] = S \tag{A1}$$

where l is the length along a field line, $\kappa T^{5/2}$ is the parallel Spitzer conductivity, T is the temperature (we take $T_e = T_i$), v is the parallel velocity, n is the density, and S gives energy sinks due to atomic processes including impurity radiation. For low Z impurities such as C, N and Ne, substantial atomic radiation is limited to a temperature range (depending on the impurity) $\sim$ 3 eV to 30 eV. At lower temperatures hydrogenic radiation (e.g. recombination) may be important, but impurity radiation is low. The temperature drops through $\sim$ 30 eV to 3 eV over a region whose length (determining the radiating volume of the SOL for impurities) is decided by intrinsic physical processes. Parallel convection increases the length of the radiation region considerably beyond what would pertain if Spitzer conduction were the only parallel transport mechanism. However, parallel convection is the dominant transport process in highly radiating divertors [36]. Thus, the length of significant impurity radiation region is determined by how far it takes for the impurities to reduce the temperature to a value where impurity radiation is no longer significant. It is very difficult for the convection velocity to exceed the sound speed, so this length is limited.

Since the parallel length for significant impurity radiation is determined by physical processes like convection, conduction etc, it does not increase as the field line length increases. Therefore, the fraction of the SOL volume where the impurities radiate decreases as the size of the machine increases. Consequently, the ratio of core to SOL impurity radiation increases with the size of the device. More quantitatively, the integral over a field line of the impurity radiation is essentially independent of the field line length, so that the volume integral over the entire SOL is proportional to the perpendicular area times the density squared. To scale current experiment to a future reactor, we use

$$P_{rad} = a_{perp}\left[\frac{n}{n_{SOL}}\right]^2\left[\frac{P_{rad}}{a_{perp}}\right]_{expt}, \quad (\text{or} P_{rad} \sim a_{perp}n^2) \tag{A2}$$

where a_{perp} is the projected area perpendicular to the field line, and $a_{perp} = 2RW_{SOL}B_{Pol}/B$ where B_{Pol}/B is the ratio of the poloidal field to the total field at the mid plane. For radiation dominated by Bremstrahlung, the radiation in the core (for a given impurity level), scales as $n_{core}V\sqrt{T}$, where T is the core temperature and V is the core volume. Hence, the ratio of the core to the SOL radiation scales as

$$\frac{P_{core}}{P_{SOL}} \sim \frac{V n_{core}^2 T}{a_{perp} n_{SOL}^2} \tag{A3}$$

For the highly radiating divertor experiments on DIII-D, the SOL width was approximately 1 cm [36]. For a similar SOL width on ITER or a reactor, the maximum SOL radiation is < 100 MW, roughly consistent with 2-D simulation results for ITER [43]. If the SOL width scaled as major radius, the SOL radiation for EU-C would be ~ 400 MW, but this would require an SOL width of $\sim$5 cm for EU-C; such a large SOL width is extremely difficult to justify. To obtain a 5 cm width, analytic expressions for the SOL width [27] require the perpendicular conductivity $\chi_{perp} \sim 120\ m^2$/sec in the SOL. Typical present experiments have $\chi_{perp} \sim 1\ m^2$/sec, and a Bohm-like scaling from present experiments to EU-C would also give a $\chi_{perp} \sim 1\ m^2$/sec - far smaller than 120 m^2/sec. It is well known that unrealistically large values of χ_{perp} would greatly ease the divertor heat loading problem, but it is precisely the implausibility of such values which makes the divertor heat loads of burning plasmas so challenging.

Finally, one learns from Eq.A1 that the impurity radiation does not increase with increasing impurity density beyond some point. In a convection dominated case, if the impurity radiation density is increased, the temperature falls more rapidly in space, so that the radiating zone decreases. In the limit of high impurity radiation, these two effects exactly compensate, so that the SOL radiation does not increase with further impurity density. This is exactly what is seen in the DIII-D experiments [35], as shown in Fig.2.

APPENDIX B: DELETERIOUS EFFECTS OF FULL DETACHMENT

The deleterious effects of full divertor detachment from plasma, which enables high radiation in the SOL, are observed in currently operating machines. In ASDEX, the H-L back transition "virtually coincides with the achievement of complete detachment" [70], but on JET, the H-L back transition can occur while the inner divertor stays attached [46]. On

DIII-D, "outboard divertor detachment is almost always accompanied by an H-L confinement transition" [71]. In JT-60U, H-mode could be obtained with full detachment, but the energy confinement was about that of an L-mode level [72].

Completely detached plasmas on JET have poor confinement, H89P < 1.5 [73]. On ASDEX, detachment coincides with a reduction in the edge pressure gradient [74]. On DIII-D, for discharges above the Greenwald limit, "a key step in accessing high densities without confinement degradation is prevention of a cold radiating zone at the x-point $\cdots$ correlated with detachment" [75]. This is also true on DIII-D below the Greenwald limit [76], and the degree of divertor closure does not significantly affect this [77]. However, JT-60U observes poor confinement near the Greenwald limit whether there is an X-point MARFE or not [78]. On TCV, density ramps are disruptively terminated by an X-point MARFE. In high density experiments on JET, full detachment could not be achieved without a disruption [79].

Reactors require confinement substantially better than L-mode [1–3, 16]. Also, no power reactor can be expected to safely operate in regimes where the probability of disruptions is anything but extremely low.

The ITER physics basis [7] concludes that operation with divertor detachment leads to confinement degradation. Based on such experimental results, ITER divertor studies correctly exclude the full divertor detachment regime from consideration for H-mode operation [13]. Another study concludes that operation in steady state requires avoiding complete detachment, which usually leads to formation of an X-point MARFE and a disruptive density limit [42].

Together, these experiments clearly show that fully detached operation is not acceptable for a reactor, even though fully detached operation potentially allows large amounts of power dissipation in the SOL.

APPENDIX C: CORE RADIATION EFFECTS ON H-MODE CONFINEMENT

Based on experimental results and theoretical reasoning, an empirical model for predicting the effects of core radiation on the loss of energy confinement is developed in this appendix. One begins with two well accepted facts: that the core radiation clearly reduces the transport power flowing through the H-mode pedestal, and that the pedestal pressure strongly affects core confinement in experiments, as predicted by stiff ion temperature gradient (ITG) models

of transport [47, 48, 80]. Thus, a reduction in pedestal pressure will lead to lower stored energy.

Numerous experimental results show that the pedestal pressure is sensitive to heating power. In C-mod, the pedestal height is found to vary roughly with the heating power P as $\sim P^{0.5}$ [81]. The total stored energy was almost linearly proportional to the pedestal pressure. Impurity radiation has also been found to strongly reduce pedestal height on C-mod [82]. A large database of ASDEX discharges [83] shows a somewhat weaker power scaling for the pedestal $\sim P^{0.2}$. The temperature profiles were found to be stiff in this data, with core temperatures multiplicatively related (approximately) to the edge temperature. In this same data set, the stored energy scaled slightly more strongly with power than the pedestal pressure, as $\sim P^{0.28}$, when using similar regression variables. Controlled parameter scans of type I ELM discharges on JET [84], where only the power is varied, find that the pedestal pressure roughly varies as $\sim P^{0.5}$, but core confinement has a weaker power scaling. For type I ELM discharges on JT-60U with high triangularity > 0.2 and high poloidal β [85], the pedestal pressure varies with input power similarl to the total stored energy (not true for low triangularity). For JET ITB shots, the pedestal pressure and the thermal stored energy were both roughly linearly proportional to the heating power (but the temperature profiles were not stiff) [69]. On DIII-D, the pedestal pressure can saturate with power for heating powers well past the H-L threshold; the pedestal depends on power only in the type III elm regime [86]. We note that reactors with core radiation fractions $\sim 85\%$ are rather close to the threshold, and so again we would expect a dependence of the pedestal on the heating power. Hence, the data clearly support a dependence of the pedestal on power.

Stiff ion temperature gradient (ITG) models supported by kinetic turbulence simulations [47, 48, 80] predict that the effect of heating power on the profile would be much stronger in the regions of lower temperature, near the top of the pedestal. Thus, the heating power flowing through the outer regions of the core and the pedestal is most pertinent for predicting the stored energy. This theoretical result, in conjunction with the data presented above, motivates the following model for the effects of core radiation: when using scaling laws to predict stored energy, the heating power should be taken to be the absorbed input heating power minus the core radiation power. We remind the reader that the plasma stored energy $W_{th} \sim P^{0.31}$ for the H-mode scaling law, and the core radiated power is conventionally not subtracted from the heating power (it is often not well known experimentally). Thus,

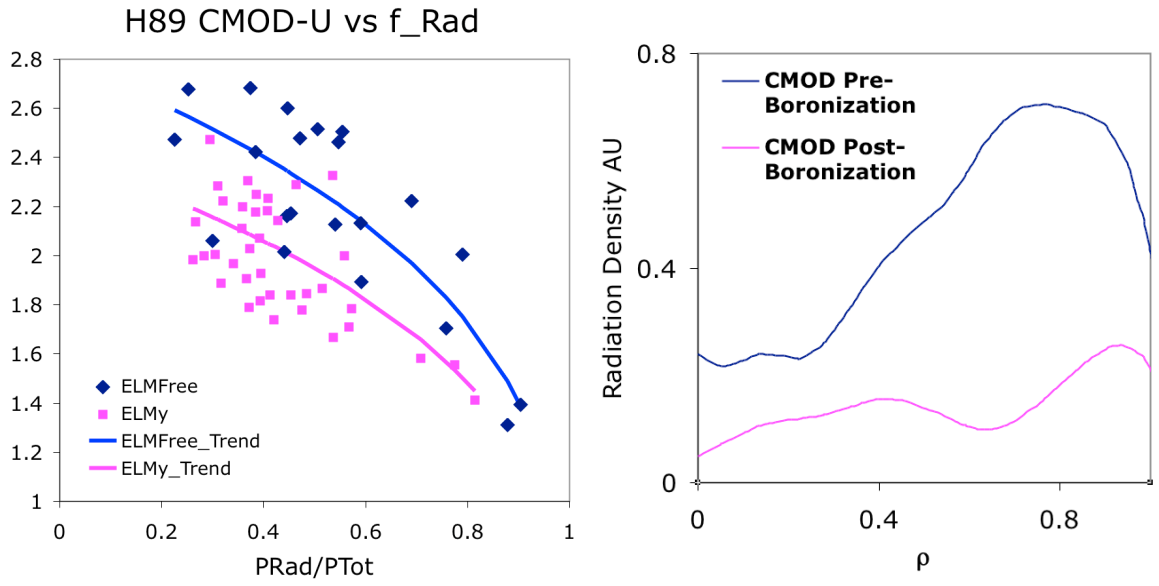

FIG. C1: a) Loss of confinement in CMOD due to core radiation. b) Core radiation profiles due mainly to Molybdenum.

to predict the stored energy with core radiation, one must reduce the stored energy by $(1 - f_{Rad,Core})^{0.31}$. This is equivalent to adjusting the H factor downward by the same amount.

We now present relevant experimental data to test this model. Experiments on C-mod demonstrate that peaked radiation profiles with large radiation fractions (due mainly to Molybdenum, a core radiator) result in a loss of confinement (Fig.C1). The data fits the trend $(1 - f_{Rad,Core})^{0.31}$ quite well.

It is interesting to realize that for discharges with high core radiation, C-mod is closer to a reactor than many other machines in a key respect: in C-mod, the ion and electron temperatures stay well equilibrated despite the cooling effect of radiation (the ratio of the classical equilibration time to the energy confinement time on C-mod is similar to a reactor). This is important when considering variations of core confinement, since a reduction in T_e relative to T_i would stabilize ion temperature gradient (ITG) modes [87], and, thus, counteract the damaging effects of radiation loss in a way that is not reactor relevant.

For temperature and density profiles relevant to a reactor in an H-mode (see Appendix D), the core radiation from seeded impurities such as Ne, Ar,Kr and Xe is peaked on axis even more strongly than is the case for C-mod [Fig.C2].

In the case of higher Z core impurities such as Kr and Xe, the radiation losses have

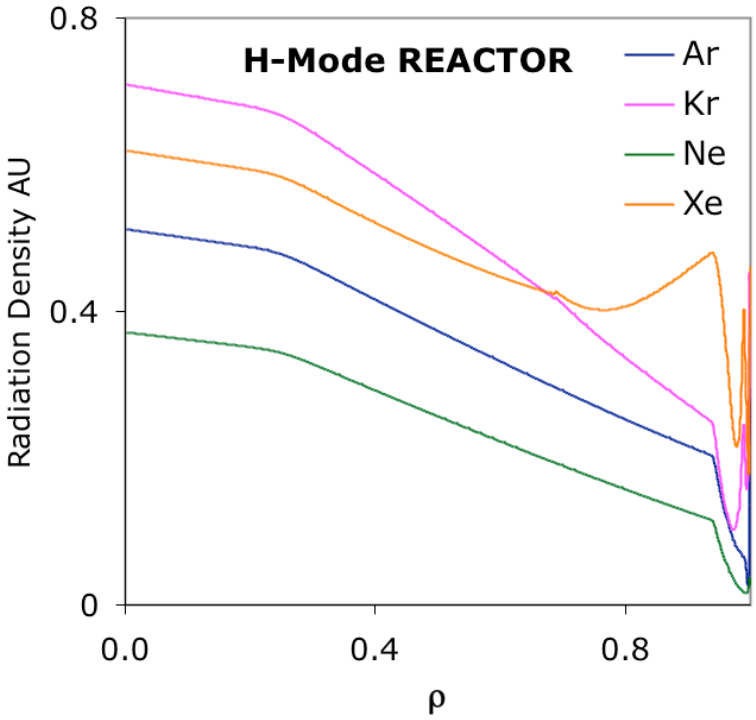

FIG. C2: Core radiation from seeded impurities such as Ne, Ar, Kr and Xe is peaked on axis even more strongly than is the case for C-mod.

a spike in the pedestal (Fig.C2) since the reactor pedestal temperature falls through the characteristic temperature for maximum radiation intensity for these high Z impurities. However, only a few percent of the radiation occurs from inside the pedestal region; most of the radiation still comes from the deep core. This is similar to what one learns from the JET data with highly radiating H-modes using Ar (much lower characteristic temperature for maximum Ar radiation is again matched by the much lower JET pedestal temperature). In Fig.C3, the H_H factors versus core radiation fraction for these cases are plotted; the data fits the trend $(1 - f_{Rad,Core})^{0.31}$ once the type I ELM and type III ELM shots are segregated. (For these parameters, the electron-ion equilibration for JET also seems reactor relevant.)

APPENDIX D: REACTOR PROFILES FOR H-MODE

To compute the profiles pertinent to an H-mode reactor, we use results from present experiments and scale them to reactor temperatures and densities. Data from hybrid H modes [61] have a ratio of central temperture to pedestal temperature of about 3, and data

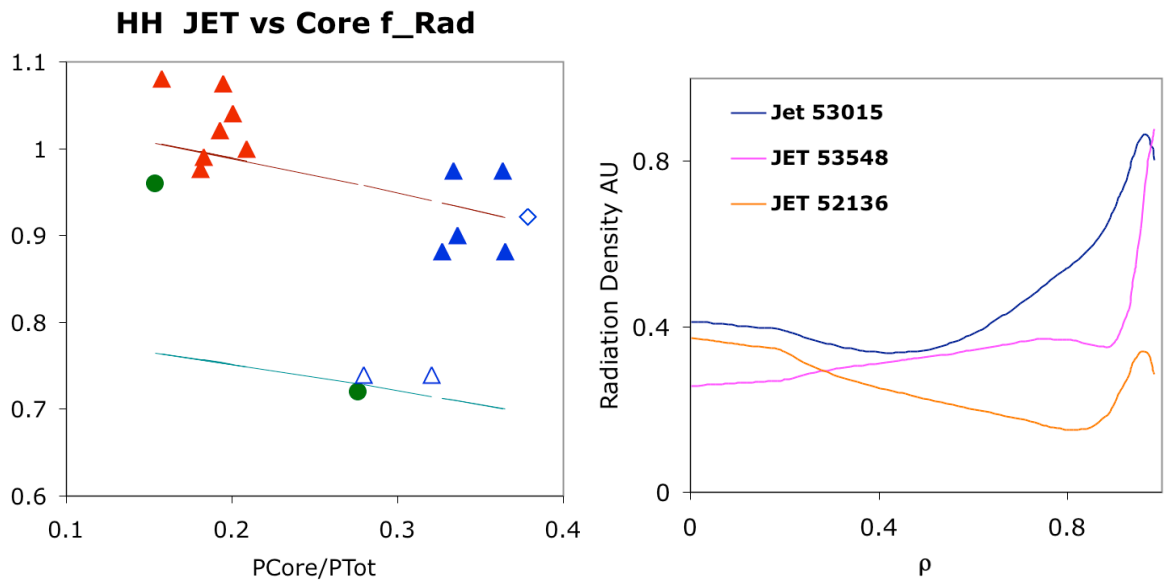

FIG. C3: a) Confinement H-factors [34] and b) radiation profiles [88] for JET impurity-seeded discharges.

from H-modes have a ratio $T_i(\rho = 0.4)/T_i(\rho = 0.8) = 1.7$. Both these results are consistent with a linear rise in the temperature from the pedestal to the center, with a central value 3 times the pedestal value. We assume such a linear profile for a reactor, and use pedestal width ~ 0.06 times the minor radius, also roughly consistent with present experiments. We choose the central temperture to match the requirements of a reactor as found in the EU-B study [16], so that the volume average temperature is 20keV. We choose a density profile which is peaked by an amount which is consistent with experimental results on JET and ASDEX [39], and which also increases linearly from the pedestal to the center.

APPENDIX E: MAGNETIC FIELD CONSTRAINTS

The engineering constraints which determine the B field in the plasma are primarily the maximum magnetic field at the superconducting coil, and the shielding distance of the superconducting coil from the thermonuclear neutrons. The field falls off as $1/R$ from the inboard superconductor to the plasma. As the major radius increases, the shielding distance stays nearly constant, so the magnetic field increases since the shield distance is a smaller fraction of the major radius. We use the sequence of major radii and magnetic field found in the EU reactor sequence [1, 16], as well as interpolations between them:

Major Radius (m)	Magnetic field (T)
< 6.2	5.6
6.8	5.8
7.5	6.0
8.05	6.45
8.6	6.9

TABLE E1: Magnetic fields for different major radii for reactors of aspect ratio = 3.

APPENDIX F: INTERNAL TRANSPORT BARRIERS AND HIGH f_{Rad}

This detailed appendix on ITB experiments provides the basis for the conclusions stated in Sec.V of the main text. The adverse effects of high $f_{Rad,Core}$ on confinement can be seen in data from JT-60U. Clearly, confinement degrades with core radiation. [89]. The core radiation fraction seems to be the principal cause of confinement degradation. As shown in Fig.F1, it is correlated with loss of confinement much better than the total or the SOL radiation. Note that this is similar to the H-mode cases in Fig.3. The dominant radiating impurities in these shots are C, Ne and Ar, and most of the core radiation is from inside the ITB. Confinement appears to degrade with increased radiation much faster than would be indicated by subtracting the radiation power from the heating power in the L-mode scaling law ITER89P [64] (see Fig.F1) The confinement degradation with radiation is roughly consistent with a linear scaling of stored energy with net heating power (heating power minus radiation). For reverse shear (RS) shots, JET has found that stored energy is roughly linear with heating power [69] and the data in Fig.F1 is roughly consistent with this. If confinement degradation with reduced heating power is stronger than indicated by using the L mode scaling law, confinement requirements for a highly radiating reactor are even more onerous.

However, in another series of JT-60U reverse shear (RS) discharges with ITBs, [67], there was no confinement degradation with core radiation fraction. Copper radiation appears to dominate in these discharges. The radiation in this group of shots is less dominated by radiation inside the ITB, as compared to the shots in Fig.F1, as indicated by soft X-ray (SXR) data. This is consistent with the radiation properties of Cu - for the same density and concentration, the radiation power at temperatures outside the ITB ($\sim$ 1 keV for these

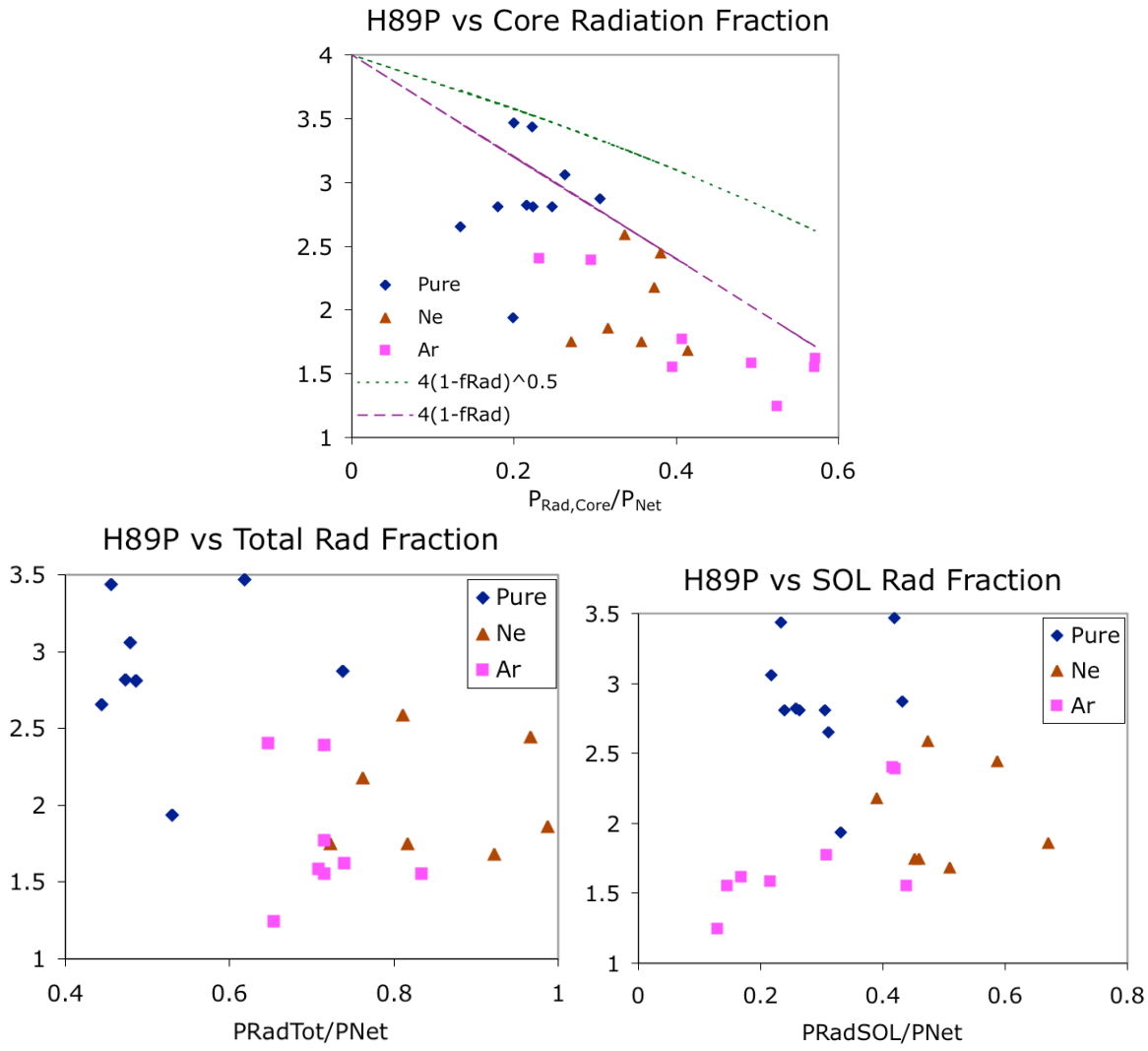

FIG. F1: The core radiation fraction (a) seems to be the principal cause of confinement degradation. It is correlated with loss of confinement much better than the total (b) or the SOL (c) radiation. Confinement deteriorates more rapidly than the L-mode scaling law indicates; the degradation is closer to linear than to the square root of core radiation fraction (a).

shots) is $\sim$ 10 times the radiation power at temperatures inside the ITB ($\sim$ 3 keV). The copper radiation pattern contrasts with impurities like C, Ne and Ar, which, for the same density and concentration, have roughly equal radiative powers for temperatures inside and outside of the ITB. For C, Ne, and Ar, these ratios are roughly 1, 2.6 and 1, respectively- much less than for Cu. Since the density inside ITBs reported on JT-60U reverse shear (RS) shots [67, 89, 90] is typically $\sim$ 3 times the density outside the ITB, the radiation inside the ITB is strongly dominant for C, Ne and Ar. However, soft X-ray (SXR) measurements

indicate that for a high radiation discharge with Cu as an impurity, only $\sim 60\%$ of the core radiation is from inside the ITB. In a Cu-seeded discharge, and for a maximum total core radiation fraction $\sim 80\%$, one then expects about half of the input power to be radiated inside the ITB. The corresponding HL factor is ~ 1.9 - only slightly above the data for the cases with $\sim 50\%$ core radiation for C, Ne and Ar shown in Fig.F1. These results suggest that high core radiation may be possible in ITB discharges with good core confinement if much of the core radiation is outside the ITB rather than inside the barrier.

At reactor temperatures the radiation rates of Cu do not favor radiation outside the ITB. In fact, for reactor conditions, all impurities are shown to radiate far more from inside than outside the ITB. Consider experimental profiles for temperature and density from high performance RS ITB shots on present devices, but with magnitude of the profiles scaled to reactor values. We choose cases on DIII-D, JET and JT-60U, with high HL (3), relatively broad pressure profiles (for good β_N) and if possible, central electron heating and data for impurity profiles. For DIII-D. we use profiles from shots which attained β_N values close to those for a reactor [63]. For JET, the choice is a high performance ITB shot 51976 [69] with among the best β_N and confinement enhancement in its category. This shot also has impurity accumulation analysis [91], and enough ICRF to give substantial central electron heating power as in a reactor-about 2/3 of the ion central heating power). For JT-60U we choose shot 41683 with strong central ECRH (over half of the total heating power), $T_i \sim T_e$, a moderately broad pressure profile, and with data analysis to obtain Ar profiles. The latter two shots also have a neoclassical collisionality very close to reactor values, so the neoclassical impurity pinch that causes accumulation should be mimic the reactor.

Three reactor studies which presume advanced tokamak operation are used to obtain volume average temperatures of 16 keV, 16 keV, and 15 keV in the reactors ARIES-RS, CREST, and EU-C [1–3, 16]. Therefore, we assume an average temperature of 16 keV, $T_i = T_e$ (T_i and T_e are highly equilibrated in these reactors), and use the average of the experimental T_i and T_e profiles. For DIII-D, JT-60 and JET, the central to pedestal temperature ratio is found to be ~ 4.5, 5, and 7, and the experimental ratios of the central density to the pedestal density to be ~ 2.8, 3.8, and 3 respectively. All shots show significant density peaking; no ITB cases were found on JET or JT-60U with large H-factors and fairly broad pressure profiles where the density was not substantially peaked.

The central temperature inside a reactor ITB is ~ 30 keV, and temperatures between the

ITB foot and the pedestal are 5-8 keV. For those temperatures, the ratio of the impurity radiation rates inside and outside the ITB for Ne, Ar, Kr, and Xe are roughly 0.8, 1, 1, and 2, respectively. These ratios are typical of the impurities in the JT-60U cases where substantial confinement degradation occurred with high radiation. There is a trend toward more favorable radiation ratios with higher Z, so we examined Hg (Z=80) as a potential impurity seed (since its vapor pressure appears high enough at reactor temperatures) - but its radiation ratio turns out to be only marginally better than Xe.

Next the fraction of the core radiation power that arises from inside the ITB foot is computed for these estimated reactor profiles. An estimate of the degree of impurity accumulation inside the ITB is needed for this purpose. On present experiments, the concentration of high Z impurities is considerably higher inside the ITB. Of course, this will increase the fraction of radiation losses inside the ITB.

We now extrapolate these results to a fusion reactor which employs Ar or Kr for core radiation. We will compute the radiation with two different assumptions - with no impurity concentration peaking inside the ITB, and with impurity peaking similar to that seen in the experiments. Recall that these shots, particularly the one on JT-60U, had considerable electron heating. Experiments find that high Z impurities are more strongly concentrated than lower Z, consistent with the stronger neoclassical impurity pinch with higher Z. In the JT-60U shot, the ratio of impurity concentration inside to outside of ITB is $\sim$ 3.5 for Ar (Z=18), and on the JET shot, the same ratio for Ni (Z=28) is $\sim$ 5. Note that Kr, Z=36, is close to Ni, Z=28. Hence, when including impurity peaking, the concentration of impurities inside and outside the ITB is taken to be the same as in the experiments described above- 3.5 for Ar and 5 for Kr.

Using these values for the reactor profiles, and varying relevant parameters, we find that over $\sim$ 90% of the radiation comes from inside the ITB for parameters consistent with attractive reactors. In Fig.F2, we vary the pressure peaking, while keeping the temperature ratio fixed at 4 and the electron density ratio at 3. The broad pressure profiles needed for good MHD beta result in very high radiation fractions inside the ITB. Next we vary the temperature ratio, for pressure peaking consistent with $\beta_N = 4$, using the relationship between peaking and β_N from Fig.5. We see that temperature ratios in the experimental range always lead to very high radiation fractions inside the ITB. At extremely high temperature ratios, however, a substantial amount of radiation can be obtained in a radiating zone close

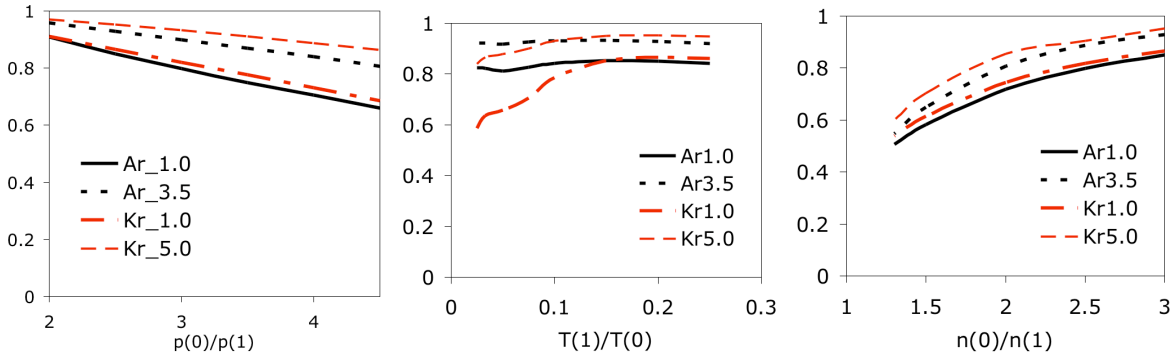

FIG. F2: Variation of the fraction of radiation inside ITB foot with profile parameters. Center and edge are denoted by 0 and 1 respectively.

to the edge and outside the ITB. Given that the central temperature is essentially fixed for a power reactor, extremely large temperature ratios imply very low edge temperatures characteristic of an L-mode edge. It has already been pointed out that experimental discharges with an L-mode edge are consistently in a low beta range not relevant to a reactor.

Finally, we vary the density peaking. As the density peaking is decreased, the impurity peaking is adjusted in a manner roughly consistent with the scaling of the neoclassical pinch term, so that the impurity concentration peaking is a power of the density peaking. (The exponent is chosen to match the experimental concentration ratios for the given experimental density peaking). We find that to obtain $\sim 60\%$ of the radiation inside the ITB, the density peaking must be very low. However, desirable experimental discharges with high β_N and broad pressure profiles show much higher density peaking.

Even if low density ratios were possible, they result in severe reduction of the bootstrap current because the bootstrap current is driven much more strongly by density gradients than by temperature gradients. We have checked the density dependence by generating high bootstrap fraction equilibria (for pressure profiles like the ones above) using the VMEC [92] code and the bootstrap codes developed for the National Compact Stellarator Experiment (NCSX) [93]. For the same pressure and q profile, the bootstrap current is almost a factor of two higher for the case with stronger density peaking. For equilibria with the β_N and aspect ratio of ARIES-RS, and a density ratio of 3, the bootstrap current was sufficient to obtain MHD parameters very close to the ARIES-RS study: a bootstrap fraction of $\sim 85\%$ and $\beta = 4.5\%$. With the same pressure profile but no density gradient, the bootstrap current fraction dropped to $\sim 42\%$. Such a fall would have a severe impact on the reactor economics.

Alternatively, the bootstrap fraction could be maintained at $\sim 85\%$ with $\beta_N = 4.5$ and no density gradient, but the plasma β is reduced by a factor of 2.2 and thus the volumetric power density would be reduced by a factor of 4.6. This would also have a severe negative effect on reactor economics. Similar results were obtained for parameters pertinent to the EU-C design. An attractive reactor, therefore, appears to demand a high density ratio.

The major result of this analysis is that the requirements for reactor-relevant high β essentially rule out the possibility of radiating a large fraction of power in the region outside the ITB. The broad pressure profiles and high bootstrap currents needed for good MHD β appear inconsistent with large radiation fractions outside the ITB, whether that radiation is in the SOL or the core. Judging from experimental results, the high confinement requirements for large radiation fractions inside the ITB are extremely demanding, (H89P = 3.6-4.6), especially when considering that a reactor will have greatly reduced velocity shear, $T_i \sim T_e$, and must have high β and high bootstrap current fraction. Since there is experimental evidence that the confinement deteriorates even more rapidly with radiation than indicated by the L-mode scaling law, the requirements could be even more daunting.

APPENDIX G: COMPONENT TEST FACILITY (CTF)

A Component Test Facility (CTF) [24] is recognized as a critical intermediate step for developing the fusion technology necessary for a reactor DEMO and certifying the performance of large components under high heat flux and neutron fluence. Obviously, to be useful and relevant, CTF should be significantly smaller (and cheaper) than a DEMO.

We now show that such a CTF is not realizable with a standard divertor (SD). In order to be small and low cost as compared to a DEMO, a CTF must have low Q$\sim$1. In order to be useful, it must also have a neutron wall loading $\sim$ 1-2 MW/m^2. So a CTF will have a P/R about the same as a reactor, and the survival of the standard divertor would require that most of the heating power be radiated from the plasma to the wall of the main chamber (outside the divertor). For a Q$\sim$1 CTF, the heat flux to the first wall must be the same as the neutron power flux$\sim$1-2 MW/m^2. However, most US and Japan reactor designs [2, 3] limit the first wall loading to less than 1 MW/m^2 and the EU designs [1] limit it to below 0.5 MW/m^2 (outside the divertor). Thus, a Q$\sim$1 CTF is not possible within engineering limits if most of the power is radiated to the first wall.

The only option for a CTF-SD (a CTF with the standard divertor) is to make it large enough that Q becomes substantially larger than 1. Together with the requirement for a large neutron wall loading, this makes a CTF-SD about as big, powerful and costly as a DEMO - only consistent with a strategy of jumping directly from ITER-FEAT to a DEMO. The risks of a DEMO failure, development delay and cost overruns are severe in this approach. Only a divertor that can withstand enough power to reduce the required radiation fraction to acceptable levels can enable operation of a small CTF with Q$\sim$1. The new X-divertor (XD) we discuss below is well suited for this task. We call a CTF with XD a CTF-XD.

In addition to providing crucial engineering data, a CTF-XD that has about the same P/R as a reactor will also directly demonstrate reliable steady state power handling at reactor relevant values (the most critical engineering problem in fusion). It will also enable development components for reliable operation in a high DT neutron fluence (the other critical engineering problem in fusion). Although a CTF-XD will not demonstrate energy gain, it will lend itself to a reliable and straightforward extrapolation to a reactor. The ability of the new X-divertor (XD) to handle higher thermal power enables us to increase Q by simply making the device bigger in size and power the historically proven reliable path for a steep climb in the Lawson parameter over the past 30 years.